SAND--90-2408

DE93 011389

SAND90-2408
TTC-1021

Unlimited Release
February 1993

A SOURCE-TERM METHOD FOR DETERMINING SPENT-FUEL TRANSPORT CASK CONTAINMENT REQUIREMENTS*

EXECUTIVE SUMMARY

Thomas L. Sanders
Kevin D. Seager
Sandia National Laboratories**
P.O. Box 5800
Albuquerque, NM 87185

Philip C. Reardon
GRAM, Incorporated
8500 Menaul Blvd., NE
Suite B-370
Albuquerque, NM 87112

*This work was performed at Sandia National Laboratories, Albuquerque, New Mexico, supported by the United States Department of Energy under Contract DE-AC04-76DP00789.

**A United States Department of Energy Facility.

DISCLAIMER

ACKNOWLEDGEMENTS

This work was performed under contract to the office of Civilian Radioactive Waste Management of the U.S. Department of Energy (DOE). The authors wish to thank N. Burrell, M. Fisher, K. Golliher, C. Kouts, W. Lake, and M. Pellechi of the DOE for supporting this work. The authors especially wish to acknowledge the contributions by the authors of the three companion reports to this Executive Summary: P. Barrett, T. Duffey, R. Einziger, H. Jordan, A. Malinauskas, W. Mings, V. Pasupathi, Y. Rashid, R. Sandoval and S. Sutherland. In addition, special thanks go to D. Ammerman and R. Glass of Sandia National Laboratories and the staff of Creative Computer Services for their review efforts and assistance in preparing this manuscript.

ABSTRACT

This Executive Summary presents the methodology for determining containment requirements for spent-fuel transport casks under normal and hypothetical accident conditions. Three sources of radioactive material are considered: (1) the spent fuel itself, (2) radioactive material, referred to as CRUD, attached to the outside surfaces of fuel rod cladding, and (3) residual contamination adhering to interior surfaces of the cask cavity. The methodologies for determining the concentrations of freely suspended radioactive materials within a spent-fuel transport cask for these sources are discussed in much greater detail in three companion reports: "A Method for Determining the Spent-Fuel Contribution to Transport Cask Containment Requirements," "Estimate of CRUD Contribution to Shipping Cask Containment Requirements," and "A Methodology for Estimating the Residual Contamination Contribution to the Source Term in a Spent-Fuel Transport Cask." Examples of cask containment requirements that combine the individually determined containment requirements for the three sources are provided, and conclusions from the three companion reports to this Executive Summary are presented.

QUALITY ASSURANCE

This work was performed under a quality level of QL-3. The applicable level-three requirements of the Sandia National Laboratories' Transportation Systems Development Division Quality Assurance Program Plan were implemented for all phases of this activity.

TABLE OF CONTENTS

This page is intentionally left blank.

LIST OF FIGURES

This page is intentionally left blank.

LIST OF TABLES

This page is intentionally left blank.

1.0 INTRODUCTION

A cask containment system can generally be designed from two perspectives: the cask and its associated hardware are either assumed to provide containment alone or the cask contents (in this case, the spent fuel) is also considered part of the containment system. The approach in which no containment benefits are taken based on the behavior of cask contents is known as a leak-tight design basis. A source-term methodology includes in the cask containment assessment the material, physical, or chemical properties of the cask contents that tend to limit or inhibit radionuclide release to that allowed under existing regulations.

The use of a source-term methodology in the analysis, design, and operation of a spent-fuel cask containment system is expected to result in safety benefits and cost savings: (1) occupational exposure can be reduced if the time required to perform containment assessment before transport is reduced, (2) fabrication expenses can be reduced, and (3) maintenance expenses can be reduced and cask service life can be extended.

The radionuclides in a spent-fuel transport cask originate from three distinct sources:

- the loaded spent fuel;
- activated corrosion and free fission products adhering to the surface of spent-fuel rods (CRUD); and
- residual loose contamination from the above sources and spent fuel pool operations that may build up in the cavity of a cask over time.

The development of a source-term methodology must consider the individual contributions of each of these sources.

Containment of cask contents by a transport cask is a function of the cask body, one or more closure lids, and various bolting, hardware, and seals associated with the cavity closure and other containment penetrations. In addition, characteristics of cask contents that impede the ability of radionuclides to move out of the cask to the external environment also provide containment. In essence, multiple release barriers exist in transport casks, and the amount of the releasable activity available in the cask is considerably lower than the total activity of its contents. A source-term approach evaluates and takes credit for the reduced magnitude of the releasable activity available in the cask by assessing the degree of barrier resistance to release provided by material characteristics and inherent barriers that impede the release of radioactive contents.

The containment requirements for radioactive material in transport casks are defined by both U.S. Nuclear Regulatory Commission (NRC) and International Atomic Energy Agency (IAEA) regulations [US90, IA90]. Both NRC and IAEA regulations allow a source-term approach in containment

evaluations. The U.S. Code of Federal Regulations, Title 10, Part 71 (10 CFR 71) requires that irradiated nuclear reactor fuel be transported in transport casks that are "designed, constructed, and prepared for shipment so that...(under specified normal conditions of transport)...there would be no loss or dispersal of radioactive contents, as demonstrated to a sensitivity of 10^{-6} A_2 per hour, no significant increase in external radiation levels, and no substantial reduction in the effectiveness of the packaging; and...(under specified hypothetical accident conditions)...there would be no escape of krypton-85 exceeding 10,000 Curies in one week, no escape of other radioactive material exceeding a total amount of A_2 in one week, and no external radiation dose rate exceeding one rem per hour at one meter from the external surface of the (transport cask)" [US90]. The quantity A_2 is a limiting activity which, if released under specific scenarios, would prevent radiological effects from exceeding a specified level consistent with radiological protection standards of the International Commission on Radiological Protection (ICRP). Values of A_2 (e.g., A_2 = 7 Ci for ^{60}Co; A_2 = 10 Ci for ^{137}Cs) are tabulated in Appendix A of 10 CFR 71; also see Safety Series 6 and Safety Series 7 by the IAEA [IA90, IA87].

Procedures generally acceptable to the NRC for assessing compliance with these provisions have been identified in Regulatory Guide 7.4 [US75]. This guide endorses the containment and leak test procedures that are specified in the American National Standards Institute (ANSI) standard ANSI N14.5 [AN87].

If direct measurement of the activity release is impractical, ANSI N14.5 states that volumetric leak rates at standard temperature and pressure conditions (cm^3/s) may be assessed instead. This leak-based containment requirement is specified in terms of the concentration of suspended radioactive material available for release from the cask (time-integrated quantities are permitted):

$$L_i = R_i/C_i \quad , \tag{1}$$

where i = N for normal conditions or A for accident conditions, L_i is the maximum permissible leak rate (cm^3/s), R_i are the regulatory limits on the rate of activity release (10^{-6} A_2 per hr for i = N, and 1 A_2 in a week for i = A), and C_i represents the time-averaged volumetric concentration of suspended particulate, liquid, or gaseous radioactive material (in Ci/cm^3 of the transport cask medium) that could escape from the containment system during transport.

Although ANSI N14.5 is quite prescriptive, little guidance is given regarding the determination of the activity concentrations C_N and C_A. When C_N and C_A cannot be definitively established, the leak-tight design criterion is required. The objective of this analysis is twofold: (1) to develop methodologies for defining C_N and C_A; and (2) to estimate appropriate containment requirements (as demonstrated by corresponding maximum permissible leak rates) for values of C_N and C_A expected during loading conditions associated with normal and accident transport environments.

Figure 1 illustrates the effect of the activity available for release from the cask on cask containment requirements in normal and accident transport conditions. The diagonal lines represent technical limit lines based on R_N and R_A for various combinations of L_i on the vertical axis and C_i on the horizontal axis. These lines are essentially constant release lines corresponding to the lower limits of unacceptable release regions to the right of each line. Limiting leak rates L_N and L_A are plotted for R_N and R_A and for varying specific source concentrations in the cask cavity, C_N and C_A, in A_2/cm^3. The leak-tight criterion shown in the horizontal line is bounding for concentrations exceeding $C_N = 3 \times 10^{-3}$ A_2/cm^3 and $C_A = 16.5$ A_2/cm^3. For smaller concentrations, ANSI N14.5 permits average gas leak rates below the sloping lines. The horizontal line represents the criterion of leak-tightness, which applies at small leak rates and is usually 10^{-7} cm^3/s.

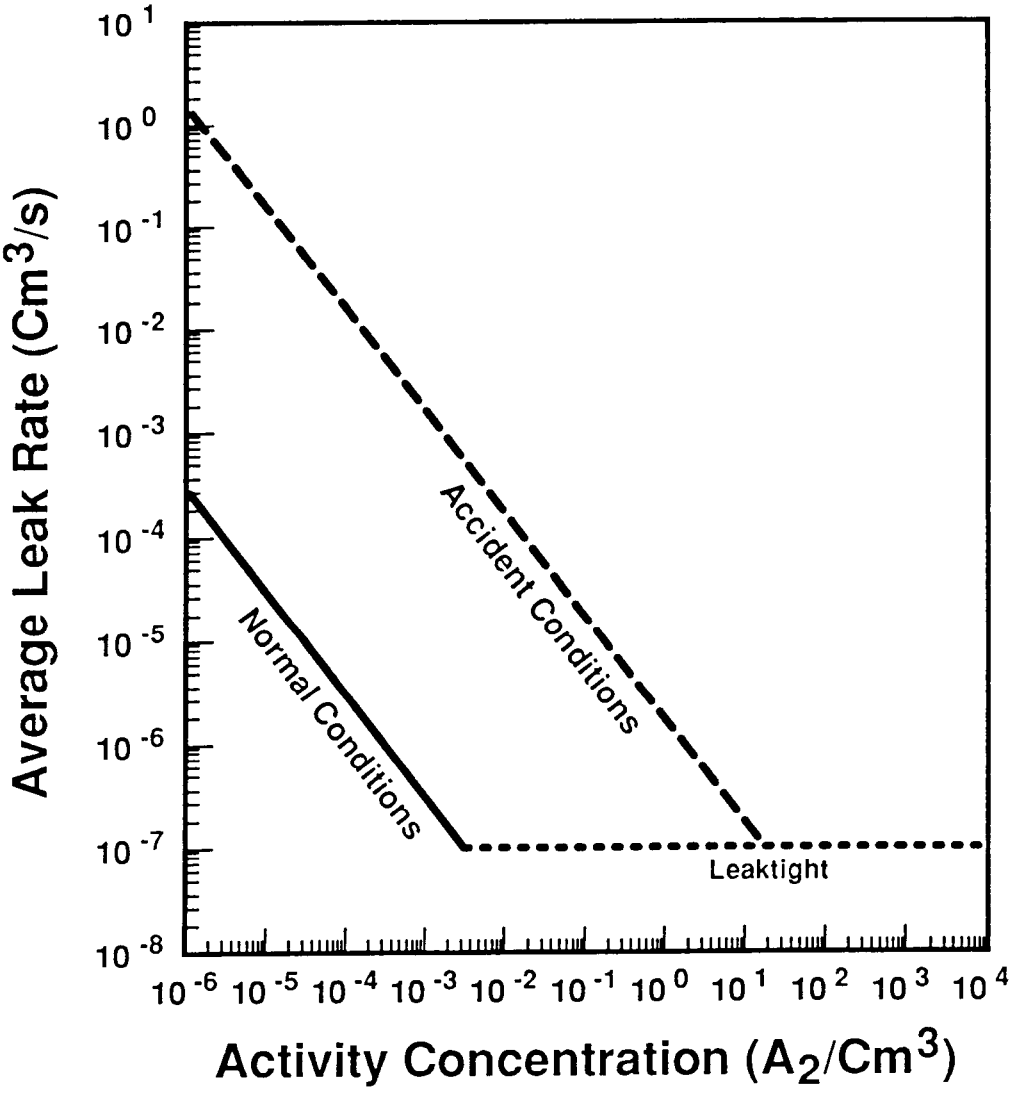

Figure 1. Limiting Average Leak Rates vs. Activity Concentration [SA91b, SA92]

The three reports accompanying this Executive Summary present a methodology for determining the concentration of freely suspended radioactive materials within a spent-fuel cask under normal and hypothetical accident transport conditions [SA92, SA91a, SA91b]. Using the relationship in Equation (1), concentrations (C_i) are converted to maximum permissible leak rates (L_i), i.e., those which provide the required degree of containment. Values of L_i are presented for both normal and accident conditions. For normal conditions, cask orientation is restricted to vertical and horizontal positions. It does not apply to the cask dropped at an angle such that the slapdown event has a drop height greater than the regulatory 0.3-m drop.

Each report treats one of three identified sources of radioactive material:

- the spent fuel (SF) itself [SA92],
- radioactive material, called CRUD, attached to the outside of fuel rod cladding [SA91a], and
- residual contamination (RC) adhering to interior surfaces of the cask cavity [SA91b].

Since the concentrations of the individual sources are additive, the maximum permissible leak rate for both normal and accident transport conditions for the combined source is written:

$$L_{total,i} = \frac{R_i}{C_{SF,i} + C_{CRUD,i} + C_{RC,i}} \quad . \tag{2}$$

The individual concentrations, $C_{SF,i}$, $C_{CRUD,i}$ and $C_{RC,i}$, determine individual leak rates $L_{SF,i}$, $L_{CRUD,i}$ and $L_{RC,i}$, when considered sole sources of activity. Expressing the individual concentrations in terms of the individual leak rates through Equation (1), Equation (2) can be rewritten in terms of the individually determined maximum permissible leak rates:

$$L_{total,i} = \frac{L_{SF,i} \times L_{CRUD,i} \times L_{RC,i}}{L_{CRUD,i}\, L_{RC,i} + L_{SF,i}\, L_{RC,i} + L_{SF,i}\, L_{CRUD,i}} \quad . \tag{3}$$

This method of combining individually determined containment requirements should only be done after all terms are converted to the same temperature and pressure conditions.

The following sections present the methodology for the three sources of radioactivity, in terms of both analysis methods and key empirical data. The results of the example analyses are for demonstration purposes only; some software must still be validated, and numerous data uncertainties reduced. Cask designers could use the current results as a sensitivity case to evaluate the future impact of this approach on their design program.

2.0 THE SPENT-FUEL METHODOLOGY

Spent fuel contains the largest potential source of releasable radioactivity [SA92]. The contribution of spent fuel to the overall maximum permissible leakage rate largely depends upon its initial pre-transport condition and on subsequent fuel rod response to transportation conditions. The type and amount of radioactive materials that may be released from the fuel rod to the cask cavity are governed by fuel cladding failure which is a function of cask and assembly designs, transport loading conditions, the transport environment, fuel irradiation histories, and other initial conditions. Since cladding failures are highly statistical events, criteria for evaluating the spent fuel source term is probabilistic, although it may depend upon deterministically derived response characteristics. Therefore, the source term methodology combines a detailed deterministic mechanical response of fuel rods and assemblies with probabilistic failure evaluations and release estimates.

Four steps were used to apply the source-term methodology to spent fuel for normal and hypothetical accident conditions of transport:

- Characterization of the dynamic environment experienced by the cask and its contents.
- Deterministic modeling of the stresses induced in spent-fuel cladding by the dynamic environment.
- Evaluation of these stresses against probabilistic failure criteria for ductile tearing and/or material fracture at generated or pre-existing cracks partially extending through the cladding wall's thickness.
- Prediction of the activity concentration in a cask cavity using knowledge of the cask void volume, the inventory of radionuclides residing in fuel-clad gaps, and estimates of the fraction of gases, volatile species, and fuel fines released.

2.1 Dynamic Cask Environments

The specific spent-fuel environments investigated and quantified were:

- The shock and vibration normally incident to over-the-road and over-the-rail transportation.
- Cask acceleration response to the 0.3-m and 9.0-m free drop impacts onto unyielding targets, and the 1.0-m drop puncture event.
- Cask and contents thermal response to 38°C ambient temperature, full solar insolation and maximum decay heat, or -40°C ambient temperature in still air and shade.
- Cask and contents thermal response to the hypothetical 30-minute duration, 800°C fully engulfing fire.

Shock and Vibration

An extensive survey of relevant shock and vibration data is presented in Appendix II of the spent-fuel report [SA92]. Simplified shock response curves and equivalent half-sine pulses were developed from the data surveyed; bounds on truck and rail vibration spectra were also developed. Figure 2 demonstrates the bounding acceleration shock response spectrum experienced by a spent-fuel cask for rail transport, assuming 3% damping, for all three axes. Superimposed on the data is a shock response spectrum for a bounding, equivalent half-sine pulse of amplitude 2.4 g and 83-ms duration for normal conditions. Similar bounding pulses were developed from the survey's data for truck shocks and rail-coupling events. The bounding truck shock pulse has an amplitude of 2.7 g and a duration of 80 ms, while the bounding rail-coupling pulse has an amplitude of 33.2 g and a duration of 30 ms for normal conditions.

The sensitivity of fuel assemblies subjected to the bounding shock and vibration loading was evaluated for potential fuel rod failure from fatigue. Analyses discussed in Appendix III of the spent-fuel report [SA92] indicate that the magnitudes of the cyclic loads induce stresses below the endurance limit of the Zircaloy cladding. Thus, existing part-wall cracks will not propagate to failure under normal transport shock and vibration loading. Shock produced by or from rail coupling events produce the largest loads on the assembly and the highest probability of rod failure from shock and vibration loading.

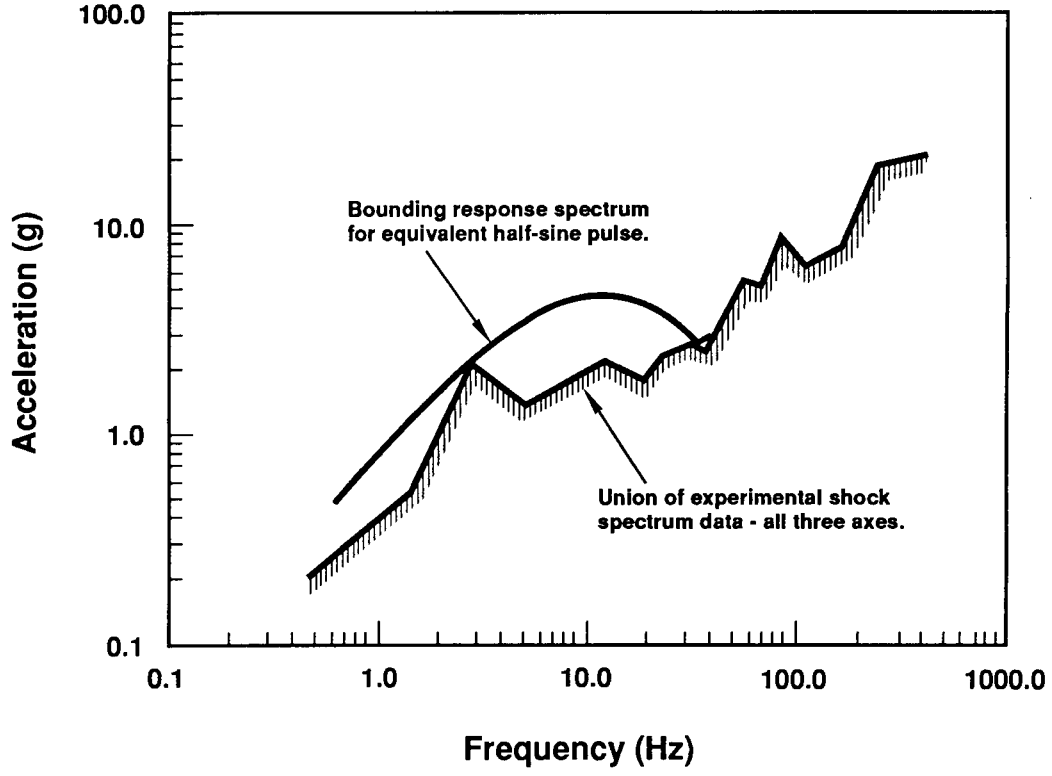

Figure 2. Bounding Half-Sine Pulse Response Spectrum for Rail Shock (excluding coupling) [SA92]

Acceleration Response

A rigid-body kinematics model was used to characterize the response of the cask and its impact limiters and transmit the resultant load history to the assemblies. This method provided acceleration vs. time history estimates for two translational and one rotational degree of freedom of the impacting cask, which was modeled as a rigid body with attached impact limiters (refer to Figure 3 for an illustration of the cask model during impact). Kinematic calculations assumed a constant crush strength for the impact limiter and were divided into an initial impact phase, a rotation phase, and a slapdown phase.

Figure 4 is an example of an acceleration history developed by the kinematic analysis. The figure shows the vertical acceleration of a 16.3- tonne lead-shielded truck cask during a half-second interval after contact, for a drop of 9.0-m at a 30° tilt angle (θ = 30° in Figure 3) onto an unyielding surface. The impact limiter had a constant crush strength of 6.89 MPa, a width of 1.22 m, and a 0.908-m radius, with a hole in the top and bottom of 24.4-cm radius (to provide a balanced design that limits peak accelerations in end drop orientations while not affecting other orientations). Such profiles were input data to the fuel response model and are cask design-dependent.

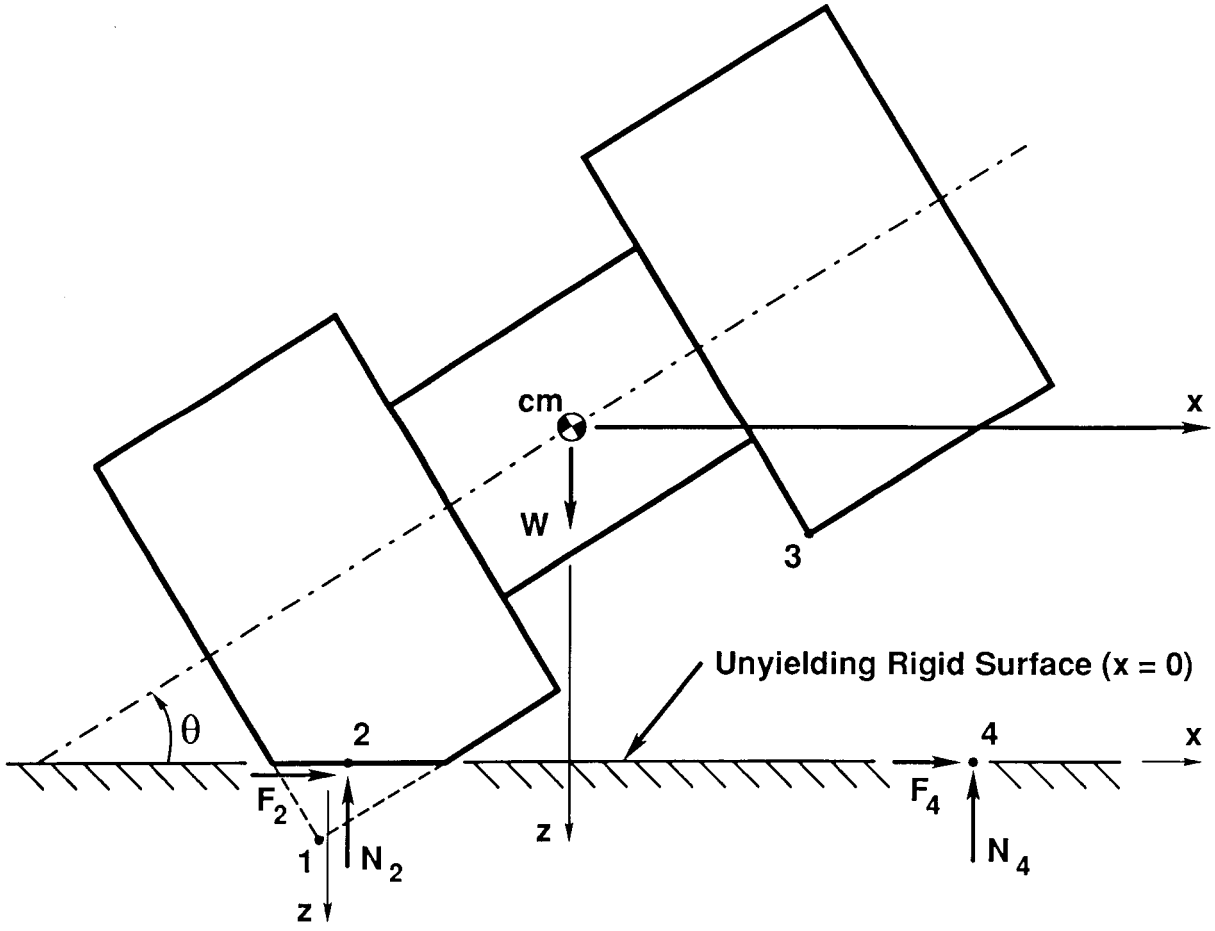

Figure 3. Rigid Body Cask Impact Model [SA92]

A total of 150 example drop conditions were analyzed involving all-steel and lead-shielded versions of both truck [assumed capacity, 1 pressurized water reactor (PWR) assembly] and rail casks (assumed capacity, twenty-one PWR assemblies). The angular dependence of peak accelerations for the same 16.3-tonne lead-shielded truck cask shown in Figure 4 is demonstrated in Figure 5 for the 9.0-m drop condition. For angles away from $\theta = 0°$ (side drop) and $\theta = 90°$ (end drop), accelerations generated during the slapdown phase greatly exceed those of the initial impact phase. For the side and end drop cases there is a single impact which results in generally higher peak accelerations being experienced. For the example casks, with an impact limiter design that included an axial hole, peak accelerations were enveloped by 100 g. Except for quantitative particulars, the examples presented here are representative; an extensive compilation of results appears in Appendix II of the spent-fuel report [SA92]. The associated impact acceleration loading from the 0.3- and 9-meter normal and accident events are the critical loading events. The probability of fuel rod breach under these events is several orders of magnitude greater than all other loading conditions.

1.0-m Drop Puncture

A 15-cm diameter mild steel punch can only exert forces up to the product of the punch cross section times the dynamic flow stress of the punch material, for a maximum force of 6.2×10^6 N. The maximum acceleration response to this force depends inversely on the cask mass. For example, a loaded NLI 1/2 cask could experience a maximum acceleration of 28.8 g; heavier casks would experience smaller accelerations. The puncture drop would produce negligible loads on the spent fuel assemblies.

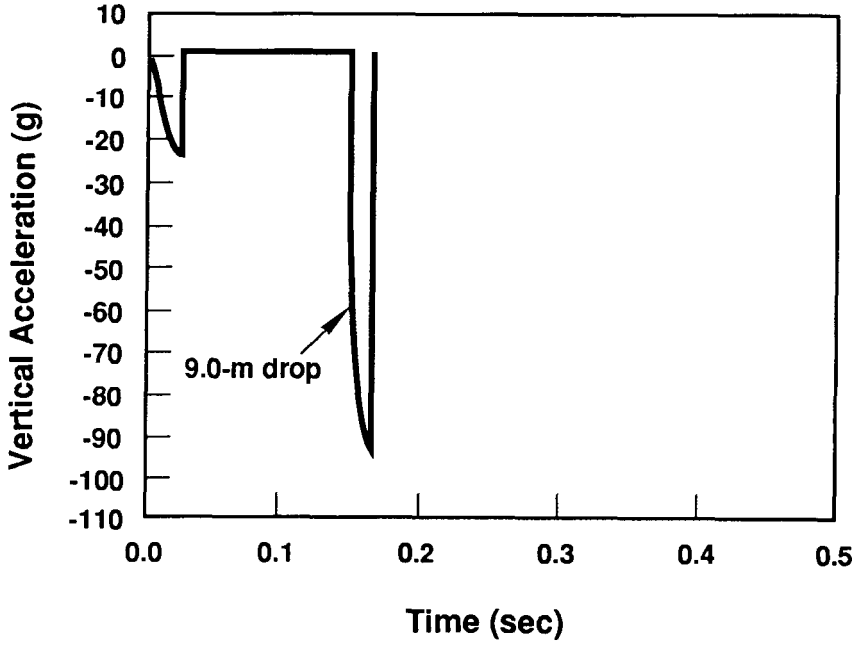

Figure 4. Vertical Acceleration vs. Time for a Lead-Shielded Truck Cask at an Impact Angle of 30° [SA92]

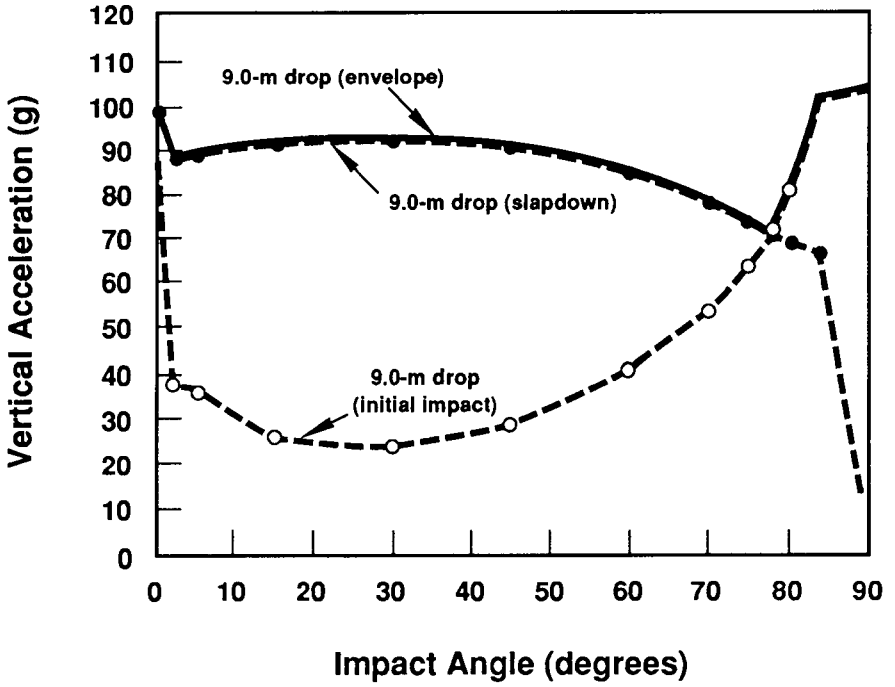

Figure 5. Peak Vertical Acceleration vs. Impact Angle for a Lead-Shielded Truck Cask in a 9.0-m Drop [SA92]

Cask Thermal Analyses

Thermal analyses were performed on two representative casks: the lead-shielded truck cask with one PWR spent-fuel assembly and the lead-shielded rail cask with an assumed payload of 21 PWR spent-fuel assemblies. Both cask concepts provide essentially the same thermal barrier as the corresponding all-steel casks. The primary purposes of these analyses were to quantify temperatures of spent fuel in the cask under both normal transport conditions and hypothetical accident transport conditions, and to contrast predicted temperatures with temperatures that are estimated to be necessary to cause thermally-induced fuel failure mechanisms such as clad rupture. The thermal analyses of the lead-shielded cask concepts were performed using the two-dimensional finite element thermal analysis code TOPAZ2D[SH86]. The thermal models are discussed in greater detail in Appendix II of the spent-fuel report [SA92].

Since tests conducted at Idaho National Engineering Laboratory (INEL) [EP86] on the Castor-V/21 PWR spent-fuel storage cask demonstrated that during long-duration tests, temperatures in the loaded cask remained below 380°C for most combinations of orientation and backfill gas, this temperature was chosen as the criterion for determining the acceptable heat load per assembly. Figure 6 shows the predicted peak fuel rod temperatures as a function of fuel assembly decay heat generation. As shown in these curves, a single 3.0-kW PWR assembly for the truck case or twenty-one 1.0-kW assemblies for the rail case result in peak temperatures that remain below the 380°C criterion.

The minimum ambient temperature of -40°C is the controlling temperature environment for the fuel since low temperatures reduce the fracture toughness of the cladding. Impact events at low temperatures increase the probability for fuel rod breach significantly. (See Section 6 of the spent fuel report [SA92] for details.)

Figure 7 presents the dynamic temperature profile near the cask centerline and the inner surface of the exterior stainless steel shell of the example truck cask under regulatory fire accident conditions. The solid curve corresponds to a fuel assembly location, while the dashed curve is at the outer radius of the lead shield. The peak temperature at the fuel location is 402°C. This temperature is well below the temperature at which thermal burst rupture of fuel rods is expected. Based on experiments performed at Battelle Memorial Institute (BMI) and Oak Ridge National Laboratory (ORNL), burst-rupture occurs at 725°C to 750°C. The mitigating influence of radiation fins and thermal barriers was not considered.

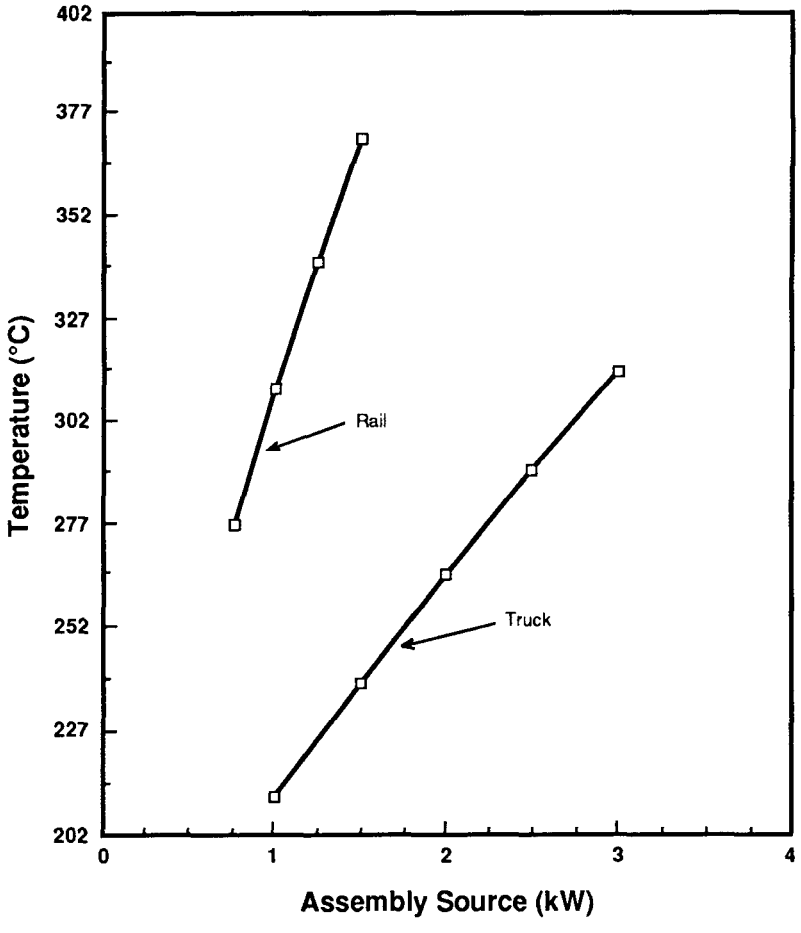

Figure 6. Predicted Peak Fuel Temperatures vs. Assembly Decay Heat Generation [SA92]

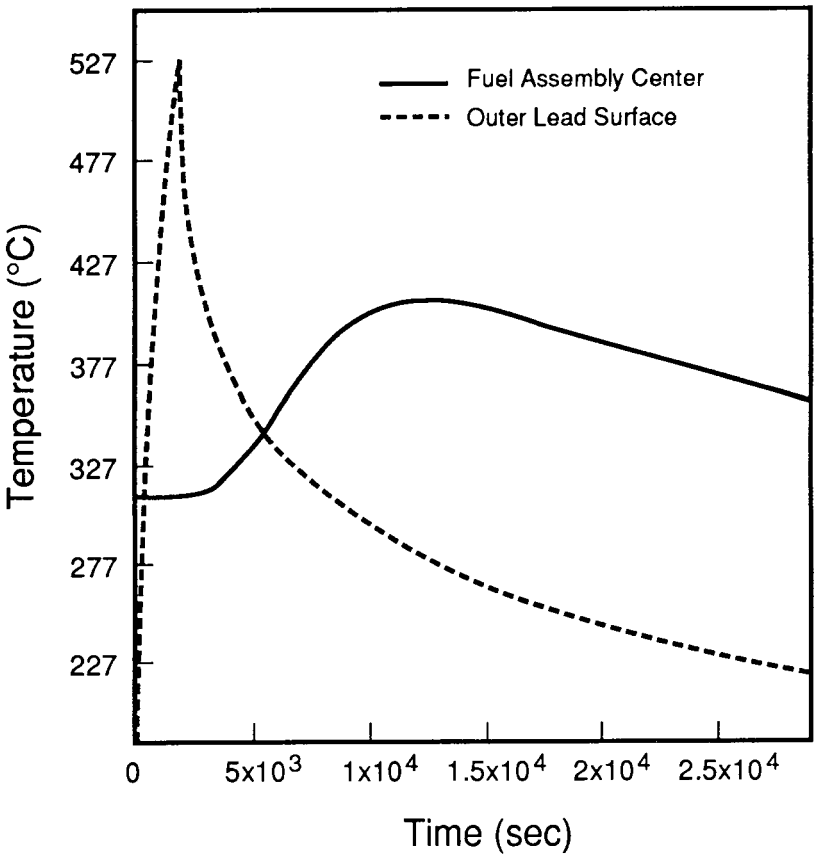

Figure 7. Predicted Regulatory Fire Accident Temperature Histories for Two Truck Cask Nodes [SA92]

2.2 Fuel Rod Response

The spent-fuel response model provides a basis for determining the probability, type, and location of fuel rod failure during regulatory normal and hypothetical accident transport conditions. The stresses induced in spent-fuel cladding by these environments were computed with deterministic geometric and material non-linear continuum finite element modeling using the general purpose code ABAQUS [HI89] and the fuel response code FREY [RA89]. Individual elements (480 or more are used to model a PWR assembly) were characterized from detailed structural models of the fuel rods, assemblies, and cask internal hardware. The analyses performed considered the spent fuel's as-transported conditions and material properties and include structural interaction between fuel baskets and assemblies, and between assembly hardware and fuel rods. Since load transfer paths from the cask to the fuel assemblies depend strongly on the drop orientation, separate structural models were developed for corner drops, end drops, and side drops. The corner drop model combines aspects of the end and side drop models to characterize initial impact and slapdown phases, respectively.

In side drops, where the amount of out-of-plane rod-to-rod interaction is negligible, an assembly is treated with a two-dimensional longitudinal slice model consisting of a single row of rods. The spacer grid structure is treated as a nonlinear spring element to account for flattening of the spacer contact springs, buckling of spacer grid frame members, and rod-to-rod contact and deflection. As rod loads increase, the cladding ovalizes until it touches the fuel pellets. Further loading is transmitted through pellet-clad contact. Rod-to-rod interactions are modeled by positioning contact spring elements along the fuel rod's length between spacer grids. The properties of these springs were developed from detailed analyses of individual spacer grid frames. In the model, tie rods (for PWR and BWR assemblies) and control rod guide tubes (for PWR assemblies) are constrained by rigid attachments at the end plates. For BWR assemblies, all other rods follow the motion of the end plates but slide through them without friction. The basket structure itself is treated through very stiff spring elements at either discrete contact points, or continuously along the length of the basket/assembly interface.

For end drop conditions, individual fuel rods are conservatively assumed to have the same response, which allows treatment of the assembly through a single rod model. This treatment is conservative because, by ignoring rod-to-rod interaction in this case, an individual rod's lateral displacement is maximized. The load path is along the axial length of a fuel rod. The fuel mass is assumed to provide no strength to the rod, but a portion is fixed to the cladding, thus causing inertial loads. For modeling of fuel rod buckling, an initial bowing profile is assumed for the rods. For fuel baskets with an open design, lateral displacements are not constrained; otherwise they are limited by the basket geometry. Basket features which constrain lateral deformation play an important role in the end drop assembly response.

Corner drops are divided into two separate events which affect opposite ends of the assembly: initial impact and slapdown. Depending on the impact angle, one of these events will dominate. Initial impact is modeled with a single rod end drop model that includes lateral and rotational loading caused by the impact angle. Assembly response during slapdown is treated by a two-dimensional model which is a modification of the side drop response model.

Example analyses were performed to demonstrate this methodology. Figures 8 and 9 illustrate side and end drop analyses of a PWR assembly. The deformed shape of the side drop analysis shows how the fuel rods deform together after the spacer grids crush. The maximum bending response is located in the bottom rods of the assembly over the basket support. The deformed shape of the end drop analysis demonstrates the large deformations of the fuel rods which are constrained by the other rods in the assembly and the basket support. The maximum strain is located at the bottom of the rod and is dominated by bending.

In addition to normal and hypothetical accident cask drop analyses, thermally induced hoop stresses at pre-existing part-wall cracks were evaluated for the fire accident. For the hypothetical fire, a thermal transient at the cladding was assumed which began at the maximum transport

temperature of 380°C and rose 150°C to a peak temperature of 530°C about 2 hrs after the 30-minute fire ended. The cladding response, evaluated using a finite element module of the FREY response code, predicted stresses well below those required for burst rupture. Propagation of those part-wall cracks was evaluated probabilistically as described in the following section.

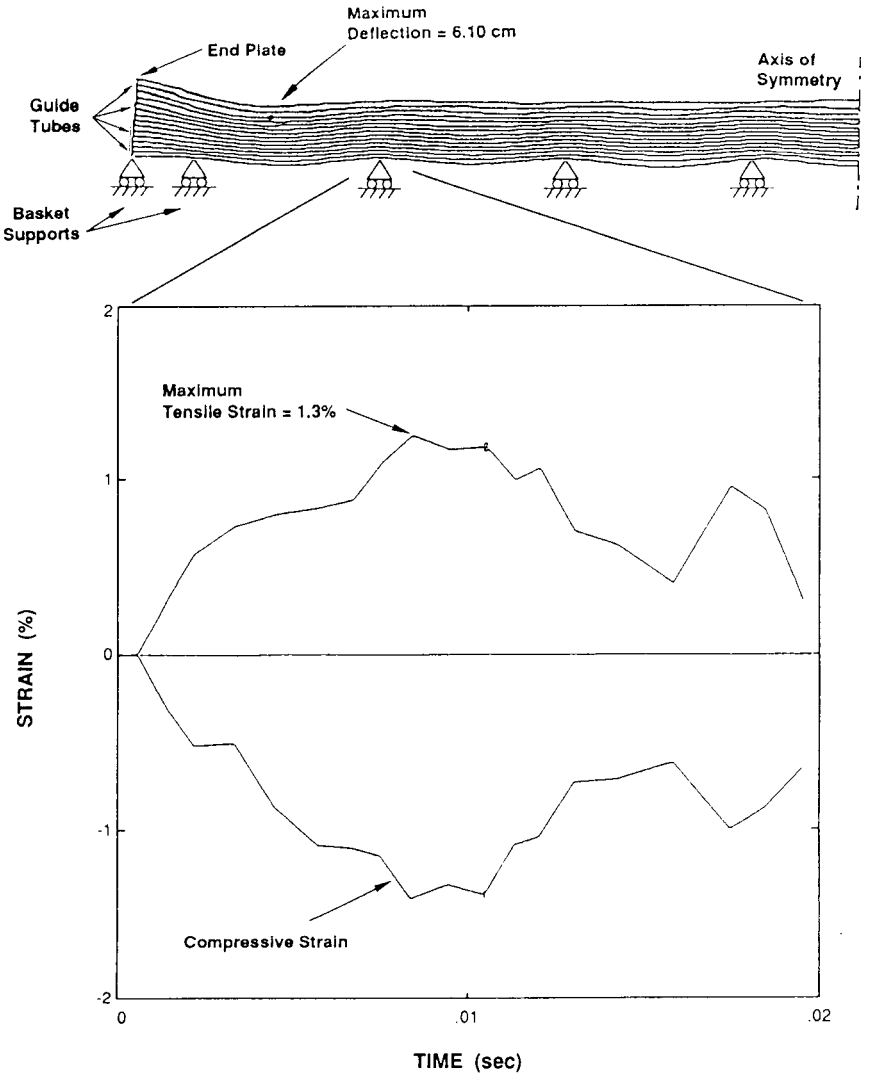

Figure 8. Deformed Shape and Selected Strain Time History for 9.0-m Side Drop [SA92]

2.3 Cladding Failure Evaluation

Cladding failure prediction is probabilistic, consistent with the observed random distribution of the failure-governing properties of spent-fuel cladding. The two material properties specifically used in the evaluation are material ductility (ε_f), related to ductile tearing from excessive strain, and fracture toughness (K_{IC}), used to determine the extension of generated or pre-existing partial (partially through the wall)

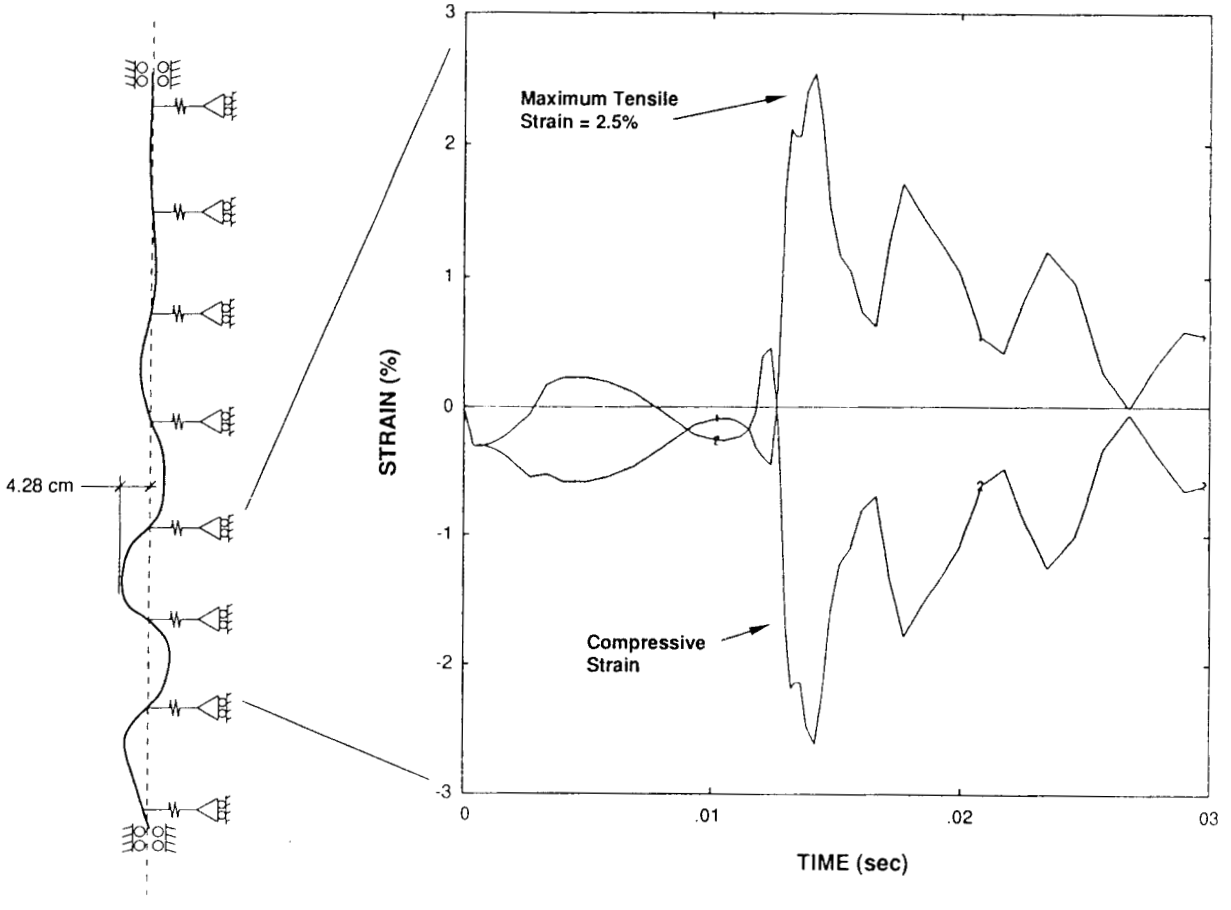

Figure 9. Deformed Shape and Selected Strain Time History for 9.0-m End Drop [SA92]

cracks. Three cladding failure modes which could occur are transverse tearing, longitudinal tearing, and rod breakage. Transverse tearing requires that longitudinal strain exceed the material ductility. Longitudinal tearing, the opening of a part-wall longitudinal crack on the inside of the cladding, requires a hoop stress intensity that exceeds the fracture toughness. The driving force for the hoop stress intensity is a pinch load arising from rod-to-rod interaction. Rod breakage is the extension of an existing transverse tear, and requires a bending stress intensity exceeding the fracture toughness of the intact material.

Thermal stresses resulting in an overpressurization of fuel cladding may cause failure by producing a thinned wall blister which expands plastically until the material's ultimate strength is exceeded. For intact

cladding, this has been observed experimentally [BU85] to occur at experimental temperatures of 725°C to 750°C, which are higher than peak values calculated for regulatory normal or accident conditions. A lower temperature mechanism exists, however, in which existing part-wall cracks extend to produce a longitudinal tear; the failure criterion in this case is the same as for mechanically induced longitudinal tears. Melting, eutectic formation and Zircaloy-water reactions all require higher temperatures and improbable secondary conditions.

Example analyses of typical BWR and PWR assemblies were performed to illustrate the fuel rod response and failure methodology. For the example BWR and PWR analyses, the GE 7 x 7 and B&W 15 x 15 assemblies were chosen, respectively. Each assembly was analyzed for impacts resulting from regulatory side, end, and corner drop loading conditions. Failure probabilities were computed for both normal and accident transport conditions.

The failure probability assessment results for the example assemblies are given in Table 1. This table includes probabilities for the three failure modes, i.e, longitudinal tearing, transverse tearing, and rod breakage. Details of these analyses are given in Appendix III of the spent fuel report [SA92]. Maximum peak tensile strains, rod-to-rod pinch forces, and conditional probabilities of failures for each failure mode were calculated for each of three axial fuel zones (end plate, spacer grid support, and midspan between spacer grids) for all applicable regulatory normal and hypothetical accident transport conditions. These probabilities were then combined to obtain the total failure probability per rod for each of the three failure modes, from which the cask fuel rod failure frequency was calculated by multiplying the highest probability of fuel rod failure by the number of rods in the transport cask.

The highest failure probability for the example GE 7 x 7 BWR assembly occurs during the initial impact phase of the 9.0-m oblique corner drop event with a failure probability of approximately 8×10^{-6} per rod per event. The methodology predicts a cask fuel rod failure frequency of approximately 0.02 for a rail cask containing fifty-two GE 7 x 7 BWR assemblies (48 fuel-bearing rods per assembly; 2,496 fuel rods total). The methodology conservatively assumes that all the rods in an assembly are subjected to the peak stress states.

The highest failure probability for the example B&W 15 x 15 PWR assembly occurs during both the slapdown phase of the 9.0-m oblique corner drop event and the 9.0-m side drop event with a failure probability of approximately 2×10^{-4} per rod per event. The methodology predicts a cask fuel rod failure frequency of approximately 0.9 for a rail cask containing twenty-one B&W 15 x 15 PWR assemblies (208 fuel-bearing rods per assembly; 4,368 fuel rods total).

For normal transport conditions, a 0.3-m side drop event results in a failure probability of approximately 4×10^{-8} per BWR rod and 3×10^{-7} per PWR rod. This translates into cask fuel rod failure frequencies of 1×10^{-4} for transport casks containing fifty-two BWR assemblies and 1.3×10^{-3} for transport casks containing twenty-one PWR assemblies, respectively.

Table 1

Summary of Example Assembly Failure Probabilities Under Normal and Hypothetical Accident Transport Conditions [SA92]

Assembly Loading Condition	Drop Angle	End Plate Tensile Strain (%)	End Plate Pinch Load (N)	End Plate No. Per Rod	Spacer Grid Support Tensile Strain (%)	Spacer Grid Support Pinch Load (N)	Spacer Grid Support No. Per Rod	Midspan Between Spacer Grids Tensile Strain (%)	Midspan Between Spacer Grids Pinch Load (N)	Midspan Between Spacer Grids No. Per Rod	Failure Probability Per Rod: Longitudinal Slit PCI Part-Wall Crack	Failure Probability Per Rod: Transverse Pinhole Rupture	Failure Probability Per Rod: Rod Breakage
GE 7 x 7 BWR													
9.0-m End Drop	90	0.342	0	1	0.166	4.45	2	0.248	0	2	2.E-10	1.E-09	2.E-13
9.0-m Corner Drop (Initial Impact)	84	2.59	0	1	0.542	703	2	0.419	841	2	8.E-10	8.E-06	2.E-06
9.0-m Corner Drop (Slapdown)	2	0.99	0	1	1.16	7940	3	0.91	0	3	1.E-06	3.E-07	2.E-07
9.0-m Side Drop	0	0.94	0	2	1.1	7562	5	0.84	0	6	2.E-06	5.E-07	7.E-07
0.3-m Normal Drop (Side Drop)	0	0.63	0	2	0.56	2900	5	0.54	0	6	1.E-08	4.E-08	1.E-09
B&W 15 x 15 PWR													
9.0-m End Drop	90	2.5	0	1	1.04	84.5	2	2.02 0.844	0 2345	1 1	6.E-10	7.E-06	8.E-07
9.0-m Corner Drop (Initial Impact)	84	2.6	0	1	0.971	72.9	2	2.08 0.546	0 3006	1 1	2.E-09	9.E-06	1.E-06
9.0-m Corner Drop (Slapdown)	2	3.47	0	1	1.37	9728	2	1.02	0	3	2.E-05	2.E-04	2.E-05
9.0-m Side Drop	0	3.3	0	2	1.3	9265	6	0.97 1.2	0	5 2	2.E-05	2.E-04	5.E-05
0.3-m Normal Drop (Side Drop)	0	1.00	0	2	0.66	3560	6	0.72	0	7	3.E-08	3.E-07	2.E-08
Fire	n/a	0.8	0	a	0.8	0	a	0.8	0	a	1.E-11	0.0[d]	0.0[d]
Normal[c] Transport	n/a	0.252	0	1	0.1	79.2	2	0.203	0	2	0.0[b]	2.E-07	2.E-12

[a]Fire analysis stress is based on part-wall crack in fuel with probability of 1 in 10,000.
[b]Stress intensity factor is less than threshold value.
[c]Normal transport is due to shock and vibration loading.
[d]These failure modes are not applicable to regulatory fire conditions.

2.4 Activity Concentrations and Leak Rates

When a breach is produced in spent-fuel cladding, gases present in the plenum at the top of individual rods, as well as in interconnecting spaces between fuel pellets, and between pellets and cladding, escape through the opening. Driven by the high-pressure differential that exists between the rod's interior and exterior, radioactive species that are mixed with the gases or become entrained in their flow will escape until the differential pressure is relaxed. There are three classes of nuclides involved: gases, e.g. ^{85}Kr, volatiles, e.g. ^{137}Cs, and any fuel fines that move with the flow.

The standard ANSI/ANS 5.4 [AN82] outlines procedures for estimating spent-fuel gap fractions for gaseous and volatile fission product elements. This standard is incorporated in the FREY computer program which was used in the present analysis to determine the total fission gas buildup in fuel-cladding gap regions. Although the standard is not in agreement with direct measurements of cesium in the gap [LO80, LO81, JO85, MA87], its methodology was conservatively modified for these analyses by essentially treating the volatile cesium isotopes as a gas and using the gap fraction of ^{85}Kr for the ^{134}Cs and ^{137}Cs isotopes. The gap fraction of tritium was assumed to be 0.5. Radionuclide inventories in fuel fines were determined by using the code ORIGEN2 [CR80, CR83], but enhanced cesium concentrations were assumed in certain situations. Based on published data [LO80, LO81, BU85], the escape of fuel fines from the cladding was taken as a direct proportion (0.003%) of the total fuel mass, and credit was taken for settling or plate-out of 90% of fines that reach the cask cavity.

Table 2 shows releases that might occur from hypothetical cladding breaches in example PWR and BWR rods, expressed in both grams and curies. These releases, if they occurred in a typical loaded truck cask, would produce activity concentrations of 0.162 A_2/m^3 for the PWR scenario, and 0.397 A_2/m^3 for the BWR scenario. These concentrations would occur only if the cladding failed. As shown in Table 1, the rod failure probability is (under regulatory conditions) 10^{-6} per event or smaller for a GE 7 x 7 BWR assembly, and 10^{-4} per event or smaller for a B&W 15 x 15 PWR assembly. The total release probability for a shipment depends on the number of transported rods.

The activity concentrations referred to can be converted to maximum permissible leak rates by applying Equation (1). The result is the containment requirement for a representative truck cask from spent fuel alone, without consideration of CRUD or residual contamination which are treated separately in the following sections. Four values result: two for normal conditions and two for accident conditions. For our truck cask example, the maximum permissible leak rate for PWR fuel under normal transport conditions is 1.72×10^{-3} cm^3/s, assuming one rod fails; for BWR fuel it is 7.00×10^{-4} cm^3/s, also assuming cladding breach in one rod. For regulatory accident conditions, the maximum permissible leak rate for the PWR scenario is 10.2 cm^3/s and for the BWR scenario it is 4.16 cm^3/s.

Table 2

Expected Radionuclide Releases From Example Light Water Reactor (LWR) Fuel Rods Due to Cladding Failure at 530°C [SA92]

Nuclide	PWR Rod[a]		BWR Rod[b]	
	g	Ci	g	Ci
^{3}H[c]	5.26E-05	5.10E-01	8.57E-05	8.31E-01
^{85}Kr[d]	3.91E-04	1.57E-01	9.54E-04	3.82E-01
^{90}Sr	3.10E-05	4.65E-03	3.55E-05	5.33E-03
^{90}Y	1.86E-08	4.66E-03	2.13E-08	5.33E-03
^{106}Ru	2.90E-07	9.86E-04	4.27E-07	1.45E-03
^{106}Rh	2.77E-13	9.86E-04	4.08E-13	1.45E-03
^{125}Sb	2.56E-07	2.64E-04	3.83E-07	3.96E-04
^{125m}Te	3.58E-09	6.44E-05	5.36E-09	9.66E-05
^{134}Cs[e]	2.82E-06	3.39E-03	5.39E-06	6.46E-03
^{137}Cs[e]	1.15E-04	1.13E-02	2.35E-04	2.31E-02
^{137m}Ba	1.22E-11	6.56E-03	1.86E-11	9.98E-03
^{144}Ce	1.80E-07	5.76E-04	1.67E-07	5.33E-04
^{144}Pr	7.63E-12	5.76E-04	7.05E-12	5.33E-04
^{144m}Pr	3.81E-14	6.91E-06	3.53E-14	6.40E-06
^{154}Eu	3.94E-06	5.91E-04	7.42E-06	1.11E-03
^{155}Eu	1.90E-07	2.66E-04	3.60E-07	5.04E-04
^{235}U	4.16E-04	8.73E-10	1.68E-04	3.53E-10
^{238}U	6.38E-02	2.10E-08	1.11E-01	3.65E-08
^{238}Pu	1.49E-05	2.54E-04	2.67E-05	4.55E-04
^{239}Pu	3.41E-04	2.11E-05	5.84E-04	3.62E-05
^{240}Pu	1.69E-04	3.88E-05	3.05E-04	7.00E-05
^{241}Pu	6.80E-05	7.48E-03	1.32E-04	1.46E-02
^{241}Am	2.54E-05	8.14E-05	5.43E-05	1.74E-04
^{244}Cm	2.53E-06	2.08E-04	1.26E-05	1.04E-03
Balance	1.66E-03	2.09E-03	4.24E-03	2.54E-03
Totals:	6.71E-02	7.12E-01	1.18E-01	1.29E+00

[a]Oconee-1 Rod 08639 irradiated to 38.2 MWD/kg U after 5-yr decay [BA83].
[b]Quad Cities-1 Rod B5A-0139 irradiated to 33.7 MWD/kg U after 5-yr decay.
[c]Gap and fuel fines, but fines are assumed to contain only 10% of original inventory.
[d]Gap and Fuel Fines.
[e]Gap and Fuel Fines. Purge (burst) release calculated (see Appendix IV of the spent fuel report [SA92]).

3.0 CRUD CONCENTRATION METHODOLOGY

The methodology for modeling the CRUD activity concentration differs from that for spent fuel. For spent fuel, due to limitations in the kind and quality of available data, detailed modeling of the cladding as a release barrier was utilized with minimal consideration given to the aerosols produced. However, for CRUD, a detailed aerosol mechanical treatment is applied to suspended CRUD particles, while there is no detailed modeling of the release barrier presented by adhesion forces.

There are two types of CRUD: a fluffy, easily removed CRUD composed mostly of hematite that is usually found on BWR rods, and a tenacious type composed of nickel-substituted spinel occurring on PWR rods. In a few BWR reactors, copper is an important constituent. Along individual rod cladding, the average to peak observed density of CRUD radioactivity is approximately two, independent of the radionuclide. The specific nuclides which are primary contributors to the CRUD total activity depend on the time since discharge from a reactor. For shipments of 5 yr or older fuel, ^{60}Co accounts for over 92% of the activity in PWR fuel and 98% of the activity in BWR fuel.

3.1 CRUD Spallation

The concentration of CRUD suspended in the cavity of a loaded spent-fuel cask depends on the amount of CRUD initially adhering to the transported assemblies, on the fraction spalled in normal and accident transport conditions, and on depletion and resuspension mechanisms acting on the suspended particles. The amount of CRUD present on spent-fuel rods has been characterized in prior work, and was updated in this effort to produce the distributions shown in Figures 10 and 11. The figures are bar graphs of the percentage of rods having different maximum activity densities, with the data referred to the fuel's original time of discharge. In both cases the distribution is bimodal, that is, two maxima are indicated. These reflect technological improvements in controlling reactor water chemistry for the nuclear industry. Most recently discharged fuel has no discernible or only slight CRUD deposits.

Quantitative details of the bonding between the CRUD and the fuel assembly surface are not known and were not discussed in this analysis. These bonds arise from Van der Walls forces between small diameter CRUD particles and atoms in the cladding surface, supplemented by stronger hydrogen bonds when water molecules are present. Surface roughness is an important factor in the overall adhesion. The CRUD report [SA91a] addresses two amounts of spallation, i.e. 15% and 100%.

3.2 Aerosol Mechanics

CRUD aerosols have a time-dependent concentration after a spallation inducing event. Contrary to the spent-fuel case, where limited data on fuel particle sizes are available, an expected particle size distribution for CRUD was developed based on one sample of fuel that is believed to be representative of BWR fuel. The distribution developed (shown in Figure 12 as the cumulative percent of particles having diameters below specific sizes) has a precise log-normal shape with mean number diameter equal to

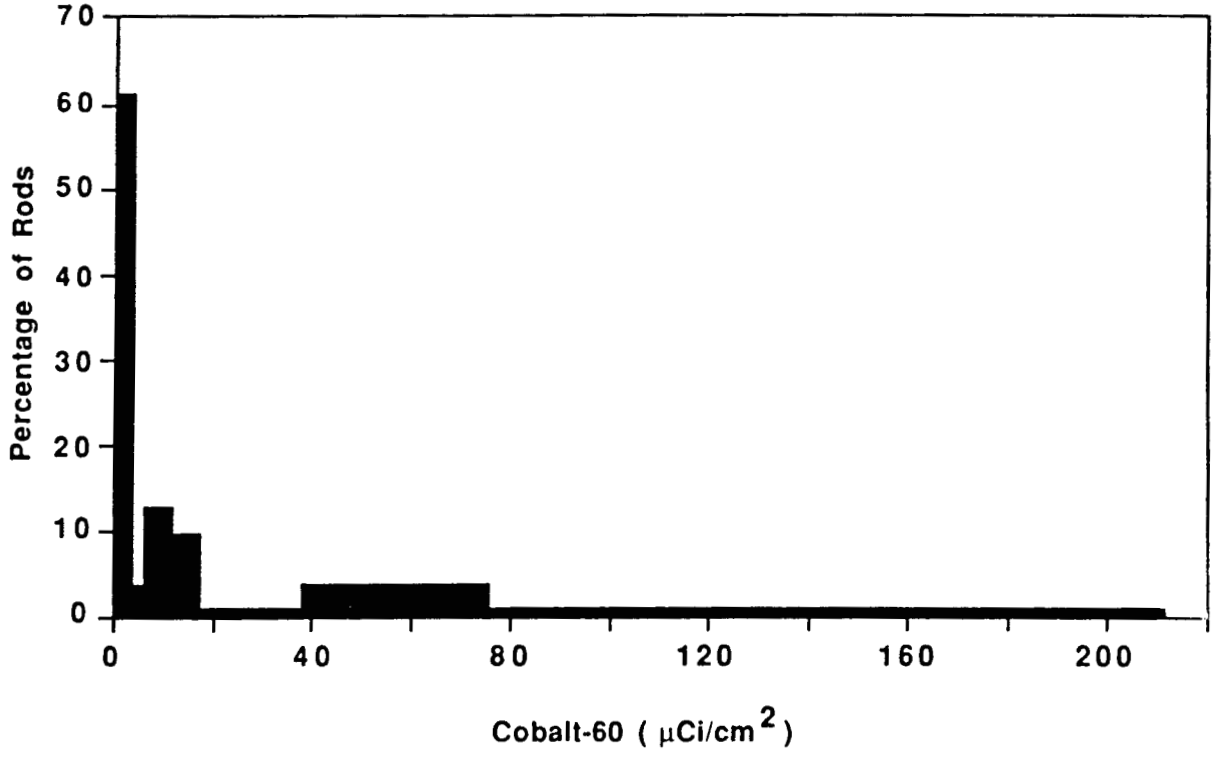

Figure 10. Distribution of PWR Spent-Fuel Rods as a Function of the Maximum Observed "Spot" Activity [SA91a]

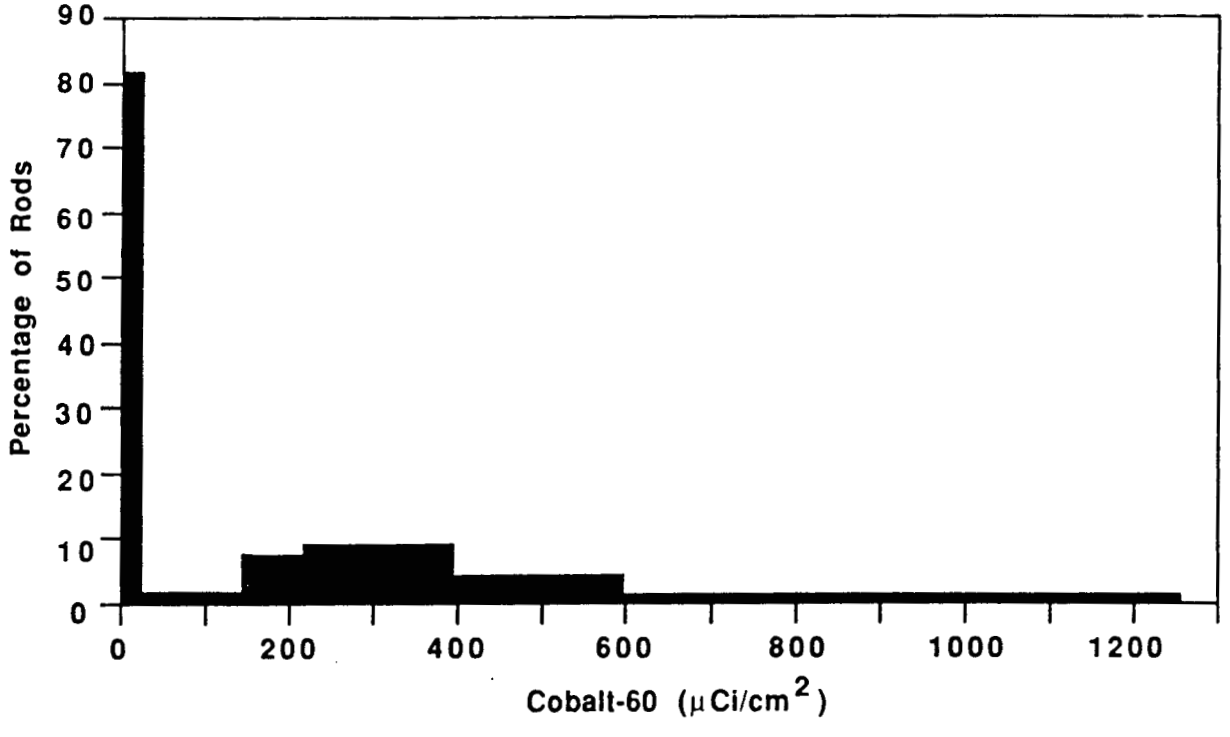

Figure 11. Distribution of BWR Spent-Fuel Rods as a Function of the Maximum Observed "Spot" Activity [SA91a]

3 μm and standard deviation of 1.87 μm. The data points are values observed in two scanning electron microscope images of Quad Cities BWR fuel cladding. The resulting curve is generally supported by measurements on CRUD scrapings taken at five other reactors.

Since a detailed distribution is available, it is possible to take credit for the behavior of aerosols inside the cask cavity. In the absence of resuspension (this assumes adhesion forces are strong and act immediately on contact with collecting surfaces), the rate of decrease in aerosol concentration is proportional to the concentration itself. The proportionality constant is the sum of three factors which individually represent the rate constants for three loss processes: (1) gravitational settling, (2) diffusive plate-out, and (3) escape from the cask by leakage.

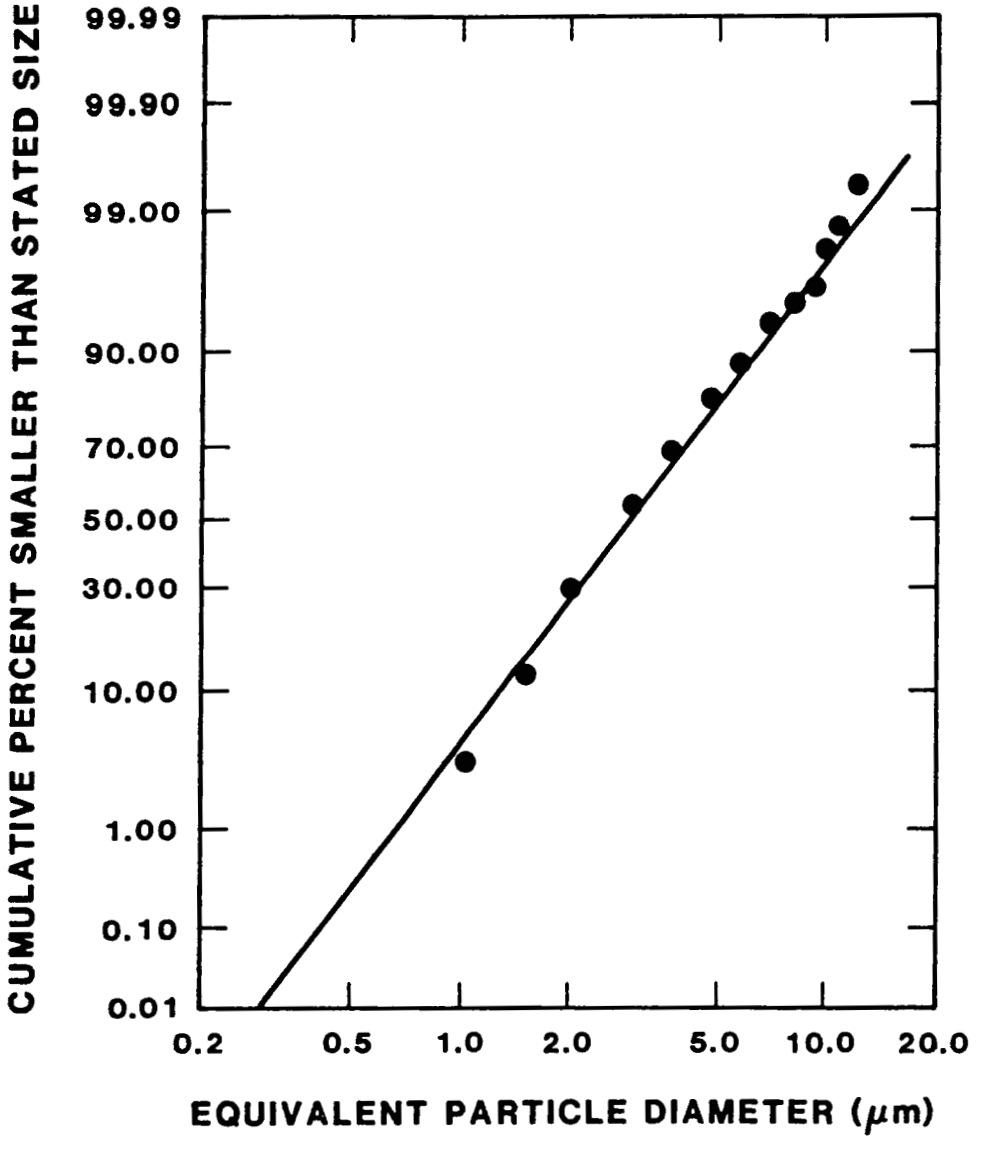

Figure 12. Particle Size Distribution by Number for CRUD From Quad Cities BWR Cladding [SA91a]

The rate constants are the reciprocals of the time it takes for the concentration to decrease by a factor of 2.718, the natural logarithm base, by one of the loss mechanisms.

The rate constant for gravitational settling is proportional to the available settling area, inversely proportional to the cask void space, and directly proportional to the settling speed. This settling speed is found from the Stokes solution for the drag on a sphere in creeping flow. The rate constant for diffusive plate-out is proportional to the total area of collecting surfaces and to the particle diffusivity, and inversely proportional to the void volume and the height of the mass transfer boundary layer at the collecting surface. The rate constant for leakage from the cask is simply the leak rate divided by the cask void volume.

The total rate constant formed by summing these three contributions shows a strong dependence on particle size, directly and indirectly through the particle volume, the particle mean free path, and the Knudson number. This implies that the number and mass particle size distributions are time-dependent, so that determination of the average concentration during an hour after spallation in normal transport or a week after an accident has to consider how these distributions change over time.

3.3 CRUD Activity Concentrations and Leak Rates

The average CRUD concentrations in a cask cavity can be expressed as the concentration immediately after spallation and initial mixing, multiplied by a Release Reduction Factor that incorporates all geometrical information on the cask volume, settling and collection areas, and the aerosols' time-varying size distribution. Table 3 presents those factors for cask and fuel geometries represented by six current generation casks, fully loaded with fuel, with CRUD characterized by the Quad Cities size distribution. Values in the table range from 7.9×10^{-4} to 2.3×10^{-3}; with smaller values resulting from relative increases in cask void space, interior settling, and plate-out areas. A range of maximum permissible leak rates is obtained when the reduction factors are applied to the cavity concentration in a truck cask, for the distributed CRUD activity shown in Figures 10 and 11. The distributions that result in the normal transport case are shown in Figure 13, for a representative truck cask with volume, settling, and plate-out areas characteristic of a loaded NLI 1/2.

As indicated in the graph, the entire population of both PWR and BWR assemblies is encompassed by a containment requirement of about 10^{-3} cm^3/s when all the CRUD is assumed to spall. When spallation is reduced to 15%, the permissible leak rates rise proportionately (see Figure 14). Appendix III of the CRUD report [SA91a] has an extensive tabulation of maximum permissible leak rates for existing truck and rail casks carrying fuel with a variety of CRUD burdens.

Table 3

Release Reduction Factors for Normal Transport
for the Quad Cities Particle Size Distribution [SA91a]

Cask Type	PWR Fuel	BWR Fuel
NLI 1/2	7.9×10^{-4}	9.6×10^{-4}
TN-8	8.3×10^{-4}	---
TN-9	----	1.1×10^{-3}
NAC-1/NSF4	1.3×10^{-3}	2.0×10^{-3}
IF-300	1.8×10^{-3}	2.2×10^{-3}
NLI 10/24	1.8×10^{-3}	2.3×10^{-3}

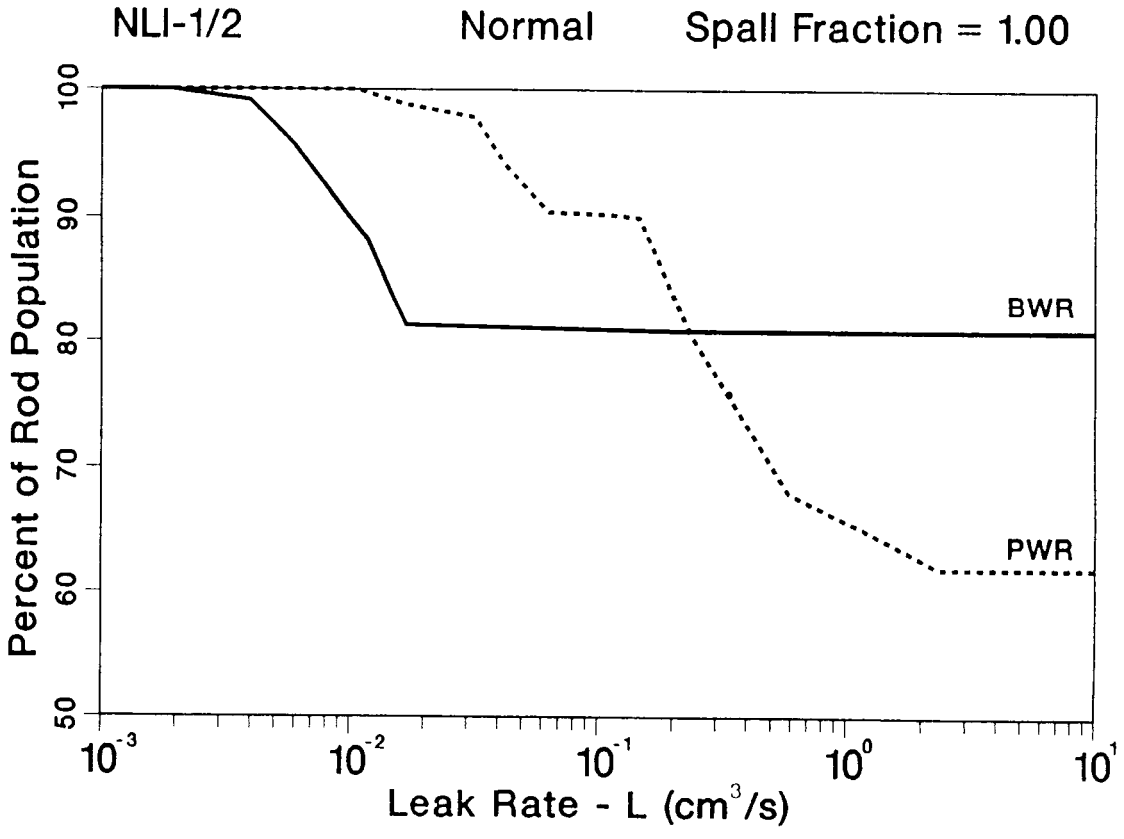

Figure 13. Distribution of Containment Requirements for a Representative Truck Cask, 100% CRUD Spallation [SA91a]

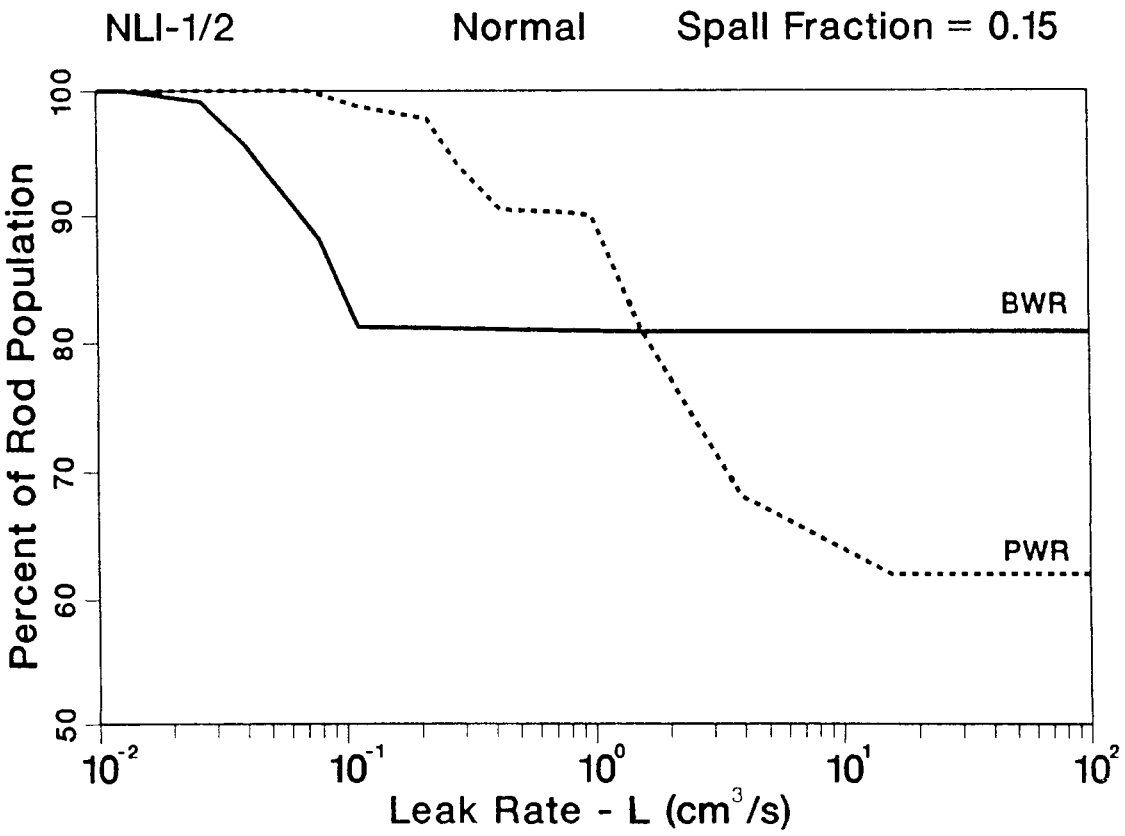

Figure 14. Distribution of Containment Requirements for a Representative Truck Cask, 15% CRUD Spallation [SA91a]

4.0 RESIDUAL CONTAMINATION METHODOLOGY

After casks have been used to transport spent fuel, their interior surfaces accumulate a residual contamination from CRUD spalled off the transported assemblies, or from immersion in storage pool water during loading and unloading of the assemblies. The residual contamination report [SA91b] (like the CRUD report) discusses the mechanisms leading to spallation but does not quantify the adhesion forces themselves, and presents previously unpublished data that clarify the amounts of residual contamination present.

Along with qualitative information derived from an extensive literature search, interior dose rate information from empty casks is given. These data were provided by Battelle Memorial Institute and the McGuire Nuclear Station of Duke Power Company. The total amount of activity on the casks' interior surfaces was derived from these data, which consist of dose rates measured at intervals along the center line of NLI 1/2- and NAC-type casks, and contact measurements near the corners of cavities in the TN-8L cask. Details of the method revealing the quantity of contamination are presented in Appendix I of the residual contamination report [SA91b], and the dose rate data provided by Battelle and Duke Power Company are presented in Appendix II.

Tables 4 and 5 present the estimated amounts of activity in curies for individual casks, identified by serial number and the measurement date. The amount of accumulated activity varies, even on the same cask from shipment to shipment, with the results ranging from about 5×10^{-4} to approximately 1 Ci of material typical of CRUD.

The example cases assume fixed spallation fractions of 15% and 100%, but treat the aerosol depletion mechanisms in detail. The same particle size distribution used for CRUD was used for residual contamination, and identical Release Reduction Factors result when the cask and fuel loading are the same.

The 1 Ci measurement is a representative but conservative amount of residual contamination, with 100% spallation in a typical truck cask loaded with PWR fuel, during normal transport. From Table 3, applying the Release Reduction Factor of 7.9×10^{-4} for a NLI 1/2 cask loaded with PWR fuel (cask void volume of 0.155 m^3) results in an average concentration of 5.1×10^{-9} Ci/cm^3. When expressed in terms of the maximum permissible leak rate, by application of Equation (1), the result is 0.38 cm^3/s. For BWR fuel, the result is 0.26 cm^3/s. An extensive set of results from example calculations, all for normal transport conditions, is presented in Table 4 of the residual contamination report [SA91b]. Maximum permissible leak rates for the less restrictive accident conditions were also calculated. The resulting permissible leak rates for accident transport conditions consistently exceed 10 cm^3/s, which implies that leaks larger than those encompassed in our modeling assumptions would still be small enough to release less than the value of A_2 of contamination in a week.

Table 4

Calculated Residual Contamination Activity Levels for NLI- and NAC-Type Casks [SA91b]

Cask Name	Date	Cask Activity (Ci)
NLI 1/2 SR# 5382	09/25/82	1.64E-01
NLI 1/2 SR# 5382	10/05/82	1.74E-02
NLI 1/2 SR# 5382-585	04/25/86	7.06E-02
NLI 1/2 SR# 5382-585	06/09/86	7.11E-02
NLI 1/2 SR# 5461	12/20/82	1.08E-02
NLI 1/2 SR# 5461	03/27/83	5.91E-04
NLI 1/2 SR# 5461	07/03/85	5.58E-01
NLI 1/2 SR# 5461	11/01/85	1.76E-02
NLI 1/2 SR# 5461	04/29/86	2.74E-02
NLI 1/2 SR# 5462-4	11/17/85	7.31E-03
NLI 1/2 SR# 5462-4	04/24/86	4.91E-02
NLI 1/2 SR# 5462-5	04/26/86	2.04E-02
NAC 1D	07/02/81	4.28E-01

Table 5

Calculated Residual Contamination Activity Levels for the TN-8L Cask [SA91b]

Cask Name	Element 1 Activity (Ci)	Element 2 Activity (Ci)	Element 3 Activity (Ci)	Total (Ci)
TN-8L (09/11/86)	3.47E-02	4.84E-02	5.16E-02	1.35E-01
TN-8L (10/28/86)	1.71E-01	1.57E-01	1.54E-01	4.83E-01
TN-8L (02/08/87)	3.28E-01	1.59E-01	3.17E-01	8.04E-01
TN-8L (03/19/87)	1.47E-01	3.62E-01	6.02E-01	1.11E+00
TN-8L (07/27/87)	2.00E-01	1.51E-01	1.22E-01	4.73E-01
TN-8L (02/24/88)	4.62E-03	1.79E-02	5.20E-03	2.77E-02

5.0 EXAMPLE CASK CONTAINMENT REQUIREMENTS

Since the calculations for the individual sources show the containment requirements to be higher for normal transport, only that case is addressed in this section. Containment requirements for the individual sources can be combined using Equation (3) to give an overall maximum permissible leak rate. For the case of truck transport of PWR fuel in normal conditions, the three individual leak rates in the examples were 1.72×10^{-3} cm^3/s due to the spent-fuel contribution, 1×10^{-3} cm^3/s due to the CRUD contribution, and 0.38 cm^3/s due to the residual contamination contribution. For the case of truck transport of BWR fuel in normal conditions, the three individual leak rates in the examples were 7.00×10^{-4} cm^3/s due to the spent-fuel contribution, 1×10^{-3}/s due to the CRUD contribution, and 0.26 cm^3/s due to the residual contamination contribution. These represent intact fuel with an extreme CRUD burden, shipped in a cask with the largest amount of residual contamination yet observed.

The maximum permissible leak rate determined for spent fuel was based on a hypothesized failure of one rod; this was shown to be an improbable event for individual rods and to increase directly in proportion to the number of rods shipped. Thus, two variations are considered in calculating the combined containment requirement for this example: (1) no failure of spent-fuel cladding, and (2) failure of a single rod. In both cases, 100% of the CRUD and residual contamination is assumed to spall. Table 6 shows a summary of the example results.

If PWR fuel cladding remains intact in the normal transport case, the containment requirement for our example is 1×10^{-3} cm^3/s. If the cladding for one rod fails, the value is 6.3×10^{-4} cm^3/s. Similarly, for the BWR case, if the fuel cladding remains intact, then the maximum permissible leak rate is again 1×10^{-3} cm^3/s, but if it fails for one rod, the value becomes 4.2×10^{-4} cm^3/s.

Table 6

Example Combined Transport Containment Requirements
During Normal Transport for a Representative Truck Cask
With High Burdens of CRUD and Residual Contamination

Fuel Type	Without Rod Failure	With Cladding Breach in One Rod
PWR	1×10^{-3} cm^3/s	6.3×10^{-4} cm^3/s
BWR	1×10^{-3} cm^3/s	4.2×10^{-4} cm^3/s

This page is intentionally left blank.

6.0 CONCLUSIONS

A number of conclusions can be drawn, based on the development of the source-term methodology and its application to a wide variety of examples. The full methodology is demonstrated in the three companion reports to this Executive Summary. The conclusions from those reports are repeated here.

6.1 Conclusions From the Spent-Fuel Report

1. The phenomena involved in determining the fuel-related source term in spent-fuel transport casks can be modeled fairly accurately on the basis of existing analytical capabilities, material properties data, and operational history information. However, some important data are sparse or lacking. Therefore, major compensating assumptions were made that affected the results in crucial ways. These assumptions were associated with numerous sensitive parameters and data uncertainties.

2. For the example cases, the failure frequency was less than one rod per rail cask accident event. An assumption of massive fuel rod failure for the containment design of spent-fuel transport casks is unrealistically very conservative.

3. Pellet-cladding interaction (PCI) incipient breaches (partial cracks) emerged as the most prominent initial fuel condition that affects the in-transport failure probability for both BWR and PWR fuels.

4. PWR spent fuel was more vulnerable to failure during transport than BWR fuel under the conditions of these analyses. The smaller PWR fuel rod diameters were mostly responsible for this condition. Rod failure as a result of initial PCI crack growth was found to be more probable for PWR fuel than BWR fuel.

5. Fuel fines, rather than the gaseous or volatile species, dominated the potentially releasable source term. However, the methodology for estimating the radionuclides contained in the fuel fines that could be purged with the gases during a cladding breach was based on a very limited amount of data. These data indicate that 0.003% of the fuel contained in an intact fuel rod is released as fuel fines following a rupture.

6. The effect of a regulatory fire following the impact test sequence will be investigated in future sensitivity analyses.

7. Oxidation and leaching radionuclide release mechanisms were not plausible events during regulatory accident conditions.

8. The fuel rod response, and consequently the failure probability, was affected by two types of uncertainties. The first was related to input parameters and can be addressed through sensitivity analyses and data development. The second, however, was related to the analytical models and was not easily

evaluated. For example, a lumped parameter (spring and mass) model, which is the predominant working model for current licensing submittals, involves much greater uncertainty than a continuum finite-element-based model such as used here.

9. Obvious gaps existed in data bases required to support this methodology at both input level and verification level. These gaps could not be totally closed through sensitivity analyses. Further experiments are required to obtain necessary data and to verify the method and results.

10. The design of cask impact limiters, fuel spacer grids, and cask basket structure significantly affected spent-fuel mechanical response.

11. For a given impulse momentum, the shape of the cask deceleration versus time history can be more important to fuel response than the amplitude of the deceleration (i.e., g-loading). This is a result of a superimposed secondary impact due to internal gaps and dynamic amplification that depend on the assembly's natural frequencies relative to the frequency of the forcing function. Therefore, the stiffness and crush strength of impact limiters that govern the shape of the deceleration-time curve could have significantly affected assembly response.

12. The higher the temperature while in transit, the lower the failure probability, provided that the burst temperature of the fuel was not exceeded. This is a result of the beneficial effects of higher temperature on cladding fracture toughness.

6.2 Conclusions From the CRUD Report

A preliminary methodology has been developed for determining the source-term activity associated with CRUD on spent-fuel assemblies. The methodology accounts for particle characteristics (such as particle size distribution) of the activity concentration inside the cask cavity, and for particle deposition due to diffusion and gravitational settling onto surfaces inside the cask cavity. Determination of the activity release to the cask cavity takes into account both normal and accident transport conditions. The effects of particle plugging of the hypothetical leak path are also addressed.

The methodology was used to estimate the CRUD-related containment requirements for typical cask geometries, assuming CRUD deposits as the only source of radioactive release from a spent-fuel shipping cask. The most current published data on CRUD composition and structure, specific activity, spallation mechanisms and fractions, and CRUD particle size were used in the calculations. For parameters where no useful quantitative data could be found, such as CRUD spallation fractions vs. impact and shock loadings characteristic of transport conditions, conservative upper-bound values were used. Example containment requirements as defined by maximum permissible leak rates were calculated assuming 5-yr-cooled spent fuel.

The results of the calculations can be summarized as follows:

1. For normal transport conditions, the maximum permissible leak rates for 5-yr-old BWR fuel shipments ranged from 1.8 x 10^{-3} cm^3/s for the TN-9 truck cask to 1.7 x 10^{-3} cm^3/s for the NLI-10/24 rail cask.

2. Similarly, for shipments of 5-yr-old PWR fuel subjected to normal transport conditions, the maximum permissible leak rates ranged from 1.4 x 10^{-2} cm^3 for the NLI-10/24 truck cask to 9.7 x 10^{-3} cm^3/s for the NLI-1/2 rail cask.

3. For the prescribed regulatory accident conditions [US90], the maximum permissible leak rates for six cask designs, regardless of orientation and for both PWR and BWR fuel, are in excess of the 10 std cm^3/s defined by ANSI N14.5 as the limiting value above which all Type B packages are exempt from design, fabrication, and assembly leak verification.

4. The maximum permissible leak rates for BWR fuel are 10 to 20 times smaller than those for PWR fuel, depending on cask type.

5. For all six casks considered for this analysis, permissible leak rates associated with normal transport conditions are the most limiting, i.e., permissible leak rates for normal transport conditions are smaller (by several orders of magnitude) than those for accident conditions.

6. The calculated maximum permissible leak rates are most sensitive to the CRUD particle size distribution of all the input parameters considered in this analysis. The effect upon maximum permissible leak rates could be a factor of 100 to 1000, depending on cask design, type of fuel, and particle size.

7. The maximum permissible leak rate values presented above are believed to be conservative upper bound estimates for CRUD releases for the following reasons.

   - The CRUD activity inventory used for this analysis conservatively assumed that the measured maximum CRUD "spot" activity is distributed uniformly over the entire surface area of the fuel assembly, even though data on axial CRUD and activity as a function of fuel rod location indicated that the average CRUD activity is significantly less than the values used in this analysis.

   - A spallation fraction of 1.0 was assumed for normal transport conditions (shock, vibration, and thermal), even though published thermal data on CRUD spallation indicated that spallation fractions of 0.15 are probably a more realistic upper bound for the normal transport conditions prescribed in 10 CFR 71.

- The assumption that CRUD spallation caused by impact, shock, or vibration occurs instantaneously, rather than at a constant rate over the release period, provides a conservative estimate of the release.

- Estimates of the effects of particle plugging of the leak path indicate that the leak path is likely to plug before the regulatory release limit of 10^{-6} A_2 of Co-60 (i.e., 7 μCi in 1 hr) is achieved.

8. These results are limited because of the scarcity of supporting experimental data in the following areas:

   - Spallation fractions for dropped or shaken spent-fuel rods.

   - Particle size distributions of spalled CRUD deposits on PWR and BWR fuel.

6.3 Conclusions From the Residual Contamination Report

A methodology has been developed for determining the activity source-term concentrations C_N and C_A in a spent-fuel transport cask associated with possible residual contamination on cask-cavity surfaces. This methodology accounts for particle characteristics (such as particle size distribution) of the activity concentration inside the cask cavity and for particle deposition due to diffusion and gravitational settling onto surfaces inside the cask cavity. (Particles in the expected size range, 1 to 10 μm, adhere strongly to surfaces to which they become attached, so resuspension is not considered.) The determination of the activity release to the cask cavity accounts for transport under both normal and accident conditions. The data used for determining potential levels of residual contaminant activity are based on actual cask shipments.

The results of the calculations can be summarized as follows:

1. For the prescribed regulatory accident conditions [US90], the maximum permissible leak rates associated with residual contaminants are likely to be well in excess of 10 std cm^3/s.

2. Measurement uncertainties present in the data that have been used limit the precision of the results to at least a factor of 3.

3. Assumptions used in our calculations that may tend to underestimate the amount of residual contamination activity available for release include the following:

   - Negligible resuspension. The initiating events in normal transport occur less frequently than once per hour, and the adhesion of settling particles is not affected by surface vibration.

   - Particle size distribution. Cask containment requirements, defined in terms of maximum permissible leak rates, are greatly affected by the particle size distribution of released

material. The effect on maximum permissible leak rates could be a factor of 100 to 1000, depending on cask design and particle size.

4. Conservative assumptions that tend to overestimate the amount of residual contamination activity available for release include the following:

   - A spallation fraction of 1.0 was used for both normal and accident conditions of transport (shock, vibration, impact, and thermal).

   - The assumption that contaminant spallation caused by impact, shock, or vibration occurs instantaneously (rather than at a constant rate over the release period) tends to overestimate the release.

   - The influence of radiation scattering on the dose rate data has not been addressed in calculating the residual contaminant burden.

   - While all activity was attributed to ^{60}Co, the data show 20 to 30 percent or more of the activity may come from other isotopes, some of which have less energetic emissions and, therefore, smaller mR/Ci conversion values.

This page is intentionally left blank.

7.0 REFERENCES

[AN82] American Nuclear Society, "Method For Calculating the Fractional Release of Volatile Fission Products From Oxide Fuel," ANSI/ANS 5.4, 1982.

[AN87] American National Standards Institute, "American National Standards for Radioactive Materials Leakage Tests on Packages for Shipment," ANSI Standard N14.5, January 16, 1987.

[BA83] Bailey, W. J., "Experience With Fuel Damage Caused by Abnormal Conditions in Handling and Transporting Operations," in Proceedings of 7th International Symposium on Packaging and Transportation of Radioactive Materials (PATRAM 83), Conference No. 830528, 1:802-807, 1983.

[BU85] Burian, R. J., K. D. Kok, R. Di Salvo, M. E. Balmert, K. R. Freeman, and A. W. Pentiman, "Response of Spent LWR Fuel to Extreme Environments," Sandia National Laboratories, Albuquerque, NM, SAND85-7213, 1985.

[CR80] Croff, A. G., "ORIGEN2: A Revised and Updated Version of the Oak Ridge Isotope Generation and Depletion Code," Oak Ridge National Laboratory, Oak Ridge, TN, 1980.

[CR83] Croff, A. G., "ORIGEN2: A Versatile Computer Code for Calculating the Nuclide Compositions and Characteristics of Nuclear Materials," Nuclear Technology, 62 (1983).

[EP86] EPRI, "The Castor-V/21 PWR Spent Fuel Storage Cask: Testing and Analyses," Electrical Power Research Institute, Palo Alto, CA, EPRI NP-4887, November 1986.

[HI89] Hibbitt, Karlsson & Sorenson, Inc., "ABAQUS: A General Purpose Finite Element Computer Program, (Providence, RI: Hibbitt, Karlsson & Sorenson, Inc., 1989).

[IA87] IAEA Safety Standards, Safety Series 7, International Atomic Energy Agency, Vienna, Austria, 1987.

[IA90] IAEA Safety Standards, Safety Series 6, International Atomic Energy Agency, Vienna, Austria, 1990.

[JO85] Johnson, L. H., S. Stroes-Gascoyne, J. D. Chen, and M. E. Attas, D. M. Sellinger, and H. G. Delaney, "The Relationship Between Fuel Element Power and the Leaching of ^{137}Cs and ^{129}I From Irradiated UO_2 Fuel," in Proceedings: ANS Meeting on Fission Product Behavior and Source Term Research, Snowbird, UT, July 15-19, 1984, Electric Power Research Institute, NP-4113-SR, pp. 15-1 to 15-2, July 1985.

[LO80] Lorenz, R. A., J. L. Collins, and A. P. Malinauskas, "Fission Product Release from Highly Irradiated LWR Fuel," NUREG/CR-0722, Oak Ridge National Laboratory, Oak Ridge, TN, 1980.

[LO81] Lorenz, R. A., J. L. Collins, M. F. Osborne, R. L. Towns, and A. P. Malinauskas, "Fission Product Release From BWR Fuel Under LOCA Conditions," NUREG/CR-1773, Oak Ridge National Laboratory, Oak Ridge, TN, 1981.

[MA87] Malinauskas, A. P., and J. T. Bell, "The Chemistry of Fission Product Iodine Under Nuclear Reactor Accident Conditions," Nuclear Safety, 28, p. 505 (1987).

[RA89] Rashid, Y. R., R. O. Montgomery, and A. J. Zangari, "FREY-01: Fuel Rod Evaluation System," Electric Power Research Institute, Palo Alto, CA, EPRI NP-3277-CCM, revised March 1989.

[SA91a] Sandoval, R. P., R. E. Einziger, H. Jordan, A. P. Malinauskas, and W. J. Mings, "Estimate of CRUD Contribution to Shipping Cask Containment Requirements," Sandia National Laboratories, Albuquerque, NM, SAND88-1358, TTC-0811, January 1991.

[SA91b] Sanders, T. L., V. Pasupathi, H. Jordan, W. J. Mings, and P. C. Reardon, "A Methodology for Estimating the Residual Contamination Contribution to the Source Term in a Spent-Fuel Transport Cask," Sandia National Laboratories, Albuquerque, NM, SAND90-2407, TTC-1020, September 1991.

[SA92] Sanders, T. L., K. D. Seager, Y. R. Rashid, P. R. Barrett, A. P. Malinauskas, R. E. Einziger, H. Jordan, T. A. Duffey, S. H. Sutherland, and P. C. Reardon, "A Method for Determining the Spent-Fuel Contribution to Transport Cask Containment Requirements," Sandia National Laboratories, Albuquerque, NM, SAND90-2406, TTC-1019, November 1992.

[SH86] Shapiro, A. B., "TOPAZ2D - A Two Dimensional Finite Element Code for Heat Transfer Analysis, Electrostatic, and Magnetostatic Problems," Lawrence Livermore National Laboratory, Livermore, CA, UCID-20824, July 1986.

[US75] U.S. Nuclear Regulatory Commission, "Leakage Tests on Packages for Shipment of Radioactive Materials," in Regulatory Guide 7.4, U.S. Nuclear Regulatory Commission, Washington, D.C., June 1975.

[US90] "Packaging and Transportation of Radioactive Material," in U.S. Code of Federal Regulations, Title 10, Part 71, revised January 1990.

DISTRIBUTION LIST

No. of Copies

175 U.S. Department of Energy
Office of Scientific and Technical Information
Attn: DOE/OSTI-4500-R74 UC-820
Oak Ridge, TN 37830

9 U.S. Department of Energy
Office of Civilian Radioactive Waste Management
Attn: R. Milner, RW-40
J. Williams, RW-421
J. Carlson, RW-431
C. Kouts, RW-431
W. Lake (5), RW-431
Routing RW-40
1000 Independence SW
Washington, DC 20585

2 U.S. Department of Energy
Naval Reactors
Attn: R. Kulbitskas, NE-60
B. K. Miles, NE-60
Routing NE-60
1000 Independence SW
Washington, DC 20585

1 U.S. Department of Energy
Northwestern On-Site Remediation Branch
Attn: J. C. Lehr, EM-44
Mail Stop EM-44
B-205
19901 Germantown Road
Germantown, MD 20585

1 U.S. Department of Energy
Office of Waste Operations
Attn: S. P. Cowan, EM-30
Mail Stop EM-30
A-214A
19901 Germantown Road
Germantown, MD 20858

1 U.S. Department of Energy
Office of Environmental Restoration
Attn: R. P. Whitfield, EM-40
Mail Stop EM-40
7A-049
1000 Independence SW
Washington, DC 20585

No. of Copies

1 U.S. Department of Energy
Division of Demonstration Testing and Evaluation
Attn: C. Cooley, EM-55
Mail Stop EM-55
7A-049
1000 Independence SW
Washington, DC 20585

1 U.S. Department of Energy
Office of Waste Operations
Attn: J. Lytle, EM-30
Mail Stop EM-30
7A-049
1000 Independence SW
Washington, DC 20585

1 U.S. Department of Energy
Division of Waste Management Projects
Attn: M. Frei, EM-34
Mail Stop EM-34
A-233
19901 Germantown Road
Germantown, MD 20585

1 U.S. Department of Energy
Attn: K. Chacey, EM-343
Mail Stop EM-343
19901 Germantown Road
Germantown, MD 20585

1 U.S. Department of Energy
Office of Environmental Restoration and Waste Management
Attn: Leo P. Duffy, Director, EM-1
Mail Stop EM-1
7A-049
1000 Independence SW
Washington, DC 20585

1 U.S. Department of Energy
Office of Technology Development
Attn: Clyde Frank, Associate Director, EM-53
7A-049
1000 Independence SW
Washington, DC 20585

No. of
Copies

6 U.S. Department of Energy
Attn: G. Boyd, EM-56
S. Denny, EM-5.11
F. Falci, EM-50.1
R. Garrison, EM-50.1
C. Miller, EM-50.1
K. Sorenson, EM-50.1
Routing EM-50.1
Washington, DC 20545

2 U.S. Department of Energy
Attn: L. Harmon, EM-32
D. Alexander, EM-53
Routing EM-53
Washington, DC 20545

1 U.S. Department of Energy
Nevada Operations Office
Attn: W. Dixon
P.O. Box 14100
Las Vegas, NV 89114-4100

3 U.S. Department of Energy
Albuquerque Operations Office
Albuquerque Headquarters
Attn: J. Bickel
K. G. Golliher
P. A. Saxman
P.O. Box 5400
Albuquerque, NM 87115

4 U.S. Department of Energy
Idaho Operations Office
Attn: W. Mings (3)
K. L. Svinicki
785 DOE Place
Idaho Falls, ID 83402

1 U.S. Department of Energy
Oak Ridge Operations Office
Attn: M. Heiskell
P.O. Box E
Oak Ridge, TN 37831

1 U.S. Department of Energy
Richland Operations Office
Attn: J. Peterson
P.O. Box 550
Richland, WA 99352

No. of
Copies

1 U.S. Department of Energy
Office of Security Regulations
Defense Programs EM-321
Attn: J. Read
Washington, DC 20545

2 AEA Technology
Winfrith Technology Center
Attn: M. Burgess
D. Martin
Dorchester, Dorset
UNITED KINGDOM DT2-8DH

1 American Nuclear Insurers
Attn: B. Einst
270 Farmington Ave.
Farmington, CT 06032

3 ANATECH Research Corporation
Attn: H. Foadian
Y. R. Rashid
R. James
PO Box 9165
LaJolla, CA 92038

1 David Andress & Associates
Inc.
Attn: D. Andress
11008 Harriet Lane
Kensington, MD 20895

1 ANEFCO, Inc.
Attn: J. Murphy
904 Ethan Allen Hwy
P.O. Box 433
Ridgefield, CT 06877

1 Argonne National Laboratory
Attn: G. Popper
9700 South Cass Ave.
Argonne, IL 60439

1 Babcock & Wilcox
Nuclear Equipment Division
Attn: T. Stevens
91 Stirling Avenue
Barberton, OH 44203

2 Babcock & Wilcox
Attn: G. Vames
R. Fisher
P.O. Box 10935
Lynchburg, VA 24506-0935

No. of
Copies

1 Battelle
Attn: V. Pasupathi
505 King Ave.
Columbus, OH 43201-2693

1 Battelle Pacific Northwest Laboratory
Attn: R. E. Einziger
PO Box 999
Richland, WA 99352

1 Bechtel National, Inc.
Attn: B. Hopkins
15740 Shady Grove Rd.
Gaithersburg, MD 20877-1454

1 Bettis Atomic Power Labs
Attn: O. Rieley
P.O. Box 79
West Mifflin, PA 15122

1 British Nuclear Fuels, Ltd.
Attn: D. Snedeker
2926 92nd Ave. E.
Puyallup, WA 98371

1 British Nuclear Fuels, Ltd.
Attn: D. Boyer
Risley Fleming House
Warrington, Cheshire
UNITED KINGDOM WA36AS

1 Carolina Power & Light Co.
Attn: R. Kunita
P.O. Box 1551
Raleigh, NC 27602

2 Center for Energy Studies
The University of Texas
Attn: D. Klein
S. Burns
10100 Burnet Rd.
Austin, TX 78758

2 Central Research Institute of Electrical Power Industry
Attn: S. Fukuda
T. Saegusa
1-6-1 Ohtemachi
Chiyodo-Ku, Tokyo
JAPAN 100

No. of
Copies

1 Chem Nuclear Systems, Inc.
Attn: R. Anderson
220 Stoneridge Dr.
Columbia, SC 29210

1 COGEMA Service Technico-Commercial Branche Retraitement
Attn: H. Bernard
2 Rue Paul Dautier
Velizy-Villacoublay
Cedex
FRANCE BP4.78141

1 Combustion Engineering
CE Power Systems
Attn: M. Falzarano
P.O. Box 500
Winsdor, CT 06095-0500

1 Commissariat a l'Energie Atomique
Department des Etudes Mecaniques et Thermiques
Service d'Etudes des Systemes
Attn: C. Vallepin
Demt Syst. CEN-Saclay
Gif-sur-Yvette
Cedex
FRANCE 91191

1 Thomas A. Duffey
P.O. Box 1239
Tijeras, NM 87059

1 Duke Power Co.
Attn: B. Rasmussen
P.O. Box 33189
Charlotte, NC 28242

1 Edison Electric Institute
Attn: C. Henkel
1111 19th Street NW
Washington, DC 20036

1 Edlow International Company
Attn: J. Edlow
1666 Connecticut Ave.
Suite 500
Washington, DC 20009

No. of
Copies

2 EG&G Idaho, Inc.
Attn: J. Clark (2)
P.O. Box 1625, MS 1540
Idaho Falls, ID 83415-1540

1 EG&G Rocky Flats Inc.
Rocky Flats Plant
Attn: H. Jordan
P.O. Box 464
Golden, CO 80402-0464

2 Electric Power Research Institute
Attn: R. Lambert
R. Williams
P.O. Box 10412
Palo Alto, CA 94303

1 Florida Power & Light Co.
Attn: D. Brodnick
P.O. Box 14000
Juno Beach, FL 33408

2 General Atomics
Attn: R. Grenier
A. Zimmer
P.O. Box 85608
San Diego, CA 92138

1 General Nuclear Systems, Inc.
Attn: P. Pacquin
220 Stoneridge Dr.
Columbia, SC 29210

2 Gesellschaft f r Nuklear-Service mbH (GNS)
Attn: H. Geiser
K. Janberg
Goethestr. 88
D-4300 Essen 1
GERMANY

6 GRAM, Inc.
Attn: P. C. Reardon (5)
R. W. Herman
8500 Menaul Blvd. NE
Suite B-370
Albuquerque, NM 87112

No. of
Copies

2 Institut de Protection et de Surete Nucleaire
Departmente d'Analyses de Surete
Commissariat a l'Energies Atomique
Attn: D. Devillers
L. Tanguy
CEN/FAR-BP No. 6
FRANCE F-92260

1 International Atomic Energy Agency
Division of Publications
Attn: R. Kelleher
Wagramerstrasse 5
P.O. Box 100
Vienna
AUSTRIA A-1400

1 E. R. Johnson Associates, Inc.
Attn: B. Teer
10461 White Granite Dr.
Suite 204
Oakton, VA 22124

1 JNT, Inc.
Attn: R. Jones
P.O. Box 1510
Los Gatos, CA 95031-1510

1 Korea Advanced Energy Research Institute
Attn: P. Han
P.O. Box 7, Daeduk-Danji
Chung-Nam
KOREA 300-31

2 Lawrence Livermore National Laboratory
University of California
Attn: L. Fischer
W. O'Connell
P.O. Box 808
Livermore, CA 94550

1 C. Marotta
1504 Columbia Ave.
Rockville, MD 20850

No. of
Copies

1 National Conference of State Legislatures
Energy, Science, and Natural Resources
Attn: B. Foster
1050 17th St., Suite 2100
Denver, CO 80265

1 National Congress of American Indians
Attn: G. Chehak
804 D Street NE
Washington, DC 20002

1 Northern States Power Co.
Attn: L. McCarten
414 Nicollet Mall
Minneapolis, MN 55401

1 Nuclear Assurance Corp.
Attn: P. Aucoin
6251 Crooked Creek Rd.
Norcross, GA 30092

1 Nuclear Energy Department
University of Missouri-Rolla
Attn: N. Tsulfanidis
Rolla, MO 65401

1 Nuclear Packaging, Inc.
Attn: R. Doman
1010 S. 336th St.
Suite 220
Federal Way, WA 98003

1 NUMARC
Attn: L. Fairobent
1776 Eye Street NW
Suite 300
Washington, DC 20006

1 NUMATEC, Inc.
Attn: P. Saverot
2550 M. Street NW
Suite 400
Washington, DC 20037

1 NUTEC
Attn: J. Rollins
1301 Hightower Trail
Suite 205
Atlanta, GA 30350

No. of
Copies

1 NUTECH Engineers
Attn: B. Thomas
145 Martinvale Lane
San Jose, CA 95119

2 Oak Ridge National Laboratory
Attn: A. Malinauskas
R. Pope
P.O. Box 2008
Oak Ridge, TN 37831-6370

1 R. Odegaarden
Attn: R. Odegaarden
1263 E. 2nd Place
Mesa, AZ 85203

1 Ontario Hydro
Research Division
Attn: J. Boag
800 Kipling Avenue
Toronto, Ontario
CANADA M8Z 5S4

1 The Ralph M. Parsons Co.
Attn: N. Ketzlach
100 W. Walnut St.
Pasadena, CA 91124

1 Pickard, Low, & Garrick Inc. (PLG)
Attn: P. Marsico
1615 M Street NW
Suite 730
Washington, DC 20036

1 Public Service Electric & Gas Co.
Attn: S. Baker
P.O. Box 236, MC N20
Hancocks Bridge, NJ 08038

1 Science Applications International Corp.
Nevada Nuclear Waste Storage Investigations
Attn: W. Andrews
Valley Bank Center
101 Convention Center Dr.
Las Vegas, NV 89109

No. of
Copies

1 Science Applications
International Corp.
Attn: T. Albert
311 Park Place Blvd.
Suite 360
Clearwater, FL 34619

1 Science Applications
International Corp.
Attn: L. Danese
P.O. Box 2501
800 Oak Ridge Turnpike
Oak Ridge, TN 37831

1 Science Applications
International Corp.
Attn: J. Stokley
1710 Goodridge Dr.
McLean, VA 22102

1 Science Applications
International Corp.
Attn: T. Hill
P.O. Box 2501
165 Mitchell Road
Oak Ridge, TN 37830

1 Siemens AG, KWU Group
Dept. U PK 13
Attn: O. Wildgruber
Hammerbacher Str. 12 + 14
Erlangen
FEDERAL REPUBLIC OF GERMANY
D-8520

1 Southern California Edison Co.
Attn: J. Ladesich
2244 Walnut Grove Ave.
Rosemead, CA 91770

1 Southern Company Services
Attn: K. Folk
P.O. Box 2625
Birmingham, AL 35202

1 Southern States Energy Board
Attn: K. Nemeth
3091 Governors Lakes Dr.
Suite 400
Norcross, GA 30071

No. of
Copies

1 Stone & Webster Energy Corp.
Attn: S. Bhatnagar
3 Executive Campus
Cherry Hill, NJ 08034

1 Svensk Karnleranslehantering
AB
Transport and AFR Storage
Division
Attn: B. Gustafsson
P.O. Box 5864
Stockholm
SWEDEN S-102 48

1 Southwest Engineering
Associates
Attn: M. Huerta
3616 Derick
El Paso, TX 79925

1 TESS Incorporated
One Federal Systems
Park Drive
Attn: B. Teer
Fairfax, VA 22023

1 Transnuclear, Inc.
Attn: M. Mason
2 Skyline Dr.
Hawthorn, NY 10532-2120

1 Union Electric
Attn: A. Passwater
P.O. Box 149, Code 470
St. Louis, MO 63166

1 Union Electric
Callaway Plant
Attn: G. Hughes
P.O. Box 620
Fulton, MO 65251

3 U.S. Council for Energy
Awareness
Attn: F. Killar
G. Russ
J. Siegel
1776 I Street, NW
Suite 400
Washington, DC 20006-2495

No. of
Copies

1 U.S. Department of
Transportation
Federal Rail Administration
RRS-32
Attn: J. Pena
400 7th Street SW
Washington, DC 20590

1 U.S. Department of
Transportation
Office of Materials
Transportation
Attn: K. Smith
400 Seventh Street SW
Washington, DC 20590

10 U.S. Nuclear Regulatory
Commission
Office of Nuclear Materials
Safety and Safeguards
Attn: R. Chappell
E. Easton
G. Gardes
A. Grella
D. Huang
H. Lee
C. MacDonald
N. Osgood
L. Wang
C. Withee
Washington, DC 20555

1 U.S. Nuclear Regulatory
Commission
Office of Nuclear Regulatory
Research
Attn: W. Lahs
NL/S-139
Washington, DC 20555

1 U.S. Nuclear Regulatory
Commission
Attn: F. Cardile
Washington, DC 20555

2 U.S. Nuclear Regulatory
Commission
Attn: G. Bidinger
L. Kopp
NMSS Mail Stop WF1-6H3
Washington, DC 20555

No. of
Copies

1 U.S. Nuclear Regulatory
Commission
Attn: C. Peterson
Mail Stop 4H3
Washington, DC 20555

1 Utility Nuclear Waste
Management Group
Attn: J. Davis
1111 19th Street NW
Washington, DC 20036

1 Virginia Power Co.
Attn: M. Smith
5000 Dominion
Glen Allen, VA 23060

1 Western Interstate Energy
Board
Attn: L. Friel
333 Quebec St.
Denver, CO 80207

1 Westinghouse Electric Corp.
Waste Technology Services
Division
Attn: B. Nair
P.O. Box 286
Madison, PA 15663-0286

1 Westinghouse Hanford Co.
Attn: C. Brown
P.O. Box 1970/MNIS T5-07
Richland, WA 99352

2 Roy F. Weston, Inc.
Attn: P. Bolton
M. Rahimi
955 L'Enfant Plaza SW
8th Floor
Washington, DC 20024

1 Wisconsin Electric Power Co.
Attn: H. Shimon
231 W. Michigan St.
Milwaukee, WI 53201

1 Yankee Atomic Electric Co.
Attn: V. Pareto
580 Main Street
Bolton, MA 01740

No. of Copies		
1	1832	R. J. Salzbrenner
1	6000	D. L. Hartley
1	6300	D. E. Miller
1	6400	N. R. Ortiz
1	6600	J. B. Woodard
1	6603	R. E. Luna
50	6603	TTC Library Attn: TTC Master File
1	6641	R. P. Sandoval
1	6641	G. S. Brown
1	6641	N. A. Russell
1	6642	G. F. Hohnstreiter
1	6642	D. J. Ammerman
1	6642	R. E. Glass
1	6642	W. L. Uncapher
1	6642	H. R. Yoshimura
10	6643	T. L. Sanders
1	6643	P. C. Bennett
1	6643	M. C. Brady
1	6643	R. I. Ewing
1	6643	S. E. Gianoulakis
1	6643	P. E. McConnell
10	6643	K. D. Seager
1	6900	T. O. Hunter
1	8523-2	Central Technical Files
5	7141	Technical Library
1	7151	Technical Publications
10	7613-2	Document Processing for DOE/OSTI

☆ U.S. GOVERNMENT PRINTING OFFICE 1992—774-122/80117